1986

Investigations of a Plasma Rotating in a Magnetic Field

Janet E. Andre

INVESTIGATIONS OF A PLASMA ROTATING IN A MAGNETIC FIELD

JANET N. ANDRE

FEBRUARY, 1986

THESIS

SUBMITTED IN PARTIAL FULFILLMENT OF THE

REQUIREMENTS FOR THE DEGREE OF MASTER OF SCIENCE

APPROVED:

Vladimir Vukoumic
Project Adviser

Department Head

Library

Rochester Institute of Technology
Rochester, New York 14623
Department of Chemistry

STATEMENT FOR GRANTING OR DENYING PERMISSION TO REPRODUCE THESIS

Title of Thesis Investigations of a Plasma Rotating in a Magnetic Field

I Janet N. Andre hereby (grant, deny) permission to the Wallace Memorial Library, of R.I.T., to reproduce my thesis in whole or in part. Any reproduction will not be for commercial use or profit.

Date November 13, 1986

ABSTRACT

A magnetically rotating electric arc of coaxial design was produced in argon with and without zinc at 1 atm. The arc was characterized in terms of temperature by varying the source conditions. The axial temperatures decreased with distance from the cathode tip and the distribution was mathematically described by $T = m * \log (x) + b$. The radial temperature distribution between the cathode and anode was determined by spectral analysis. The most homogeneous conditions with an argon/zinc plasma varied by approximately 4 % and could be applied in spectrochemical analysis. A steady state condition in terms of the frequency of rotation and gas and plasma temperatures was observed under all conditions with time. Equilibrium concentrations of species calculated with the computer program SOLGAS were found to be useful in predicting prevailing chemical conditions for a wide range of temperatures.

TABLE OF CONTENTS

VII. APPENDIX

LIST OF FIGURES

LIST OF TABLES

I. INTRODUCTION

In analytical emission spectroscopy, line spectra, emitted by atoms and ions, are used for detecting the presence of elements and determining their concentrations. In some instances, particularly in flame-emission spectroscopy, band spectra, emitted by molecules, also serve this purpose. To obtain line or band spectra, liquid and solid samples must be converted into vapor, which is energized in the source. The spectrum obtained for a given element is influenced by the properties and composition of the sample and the nature of the excitation source.

The source both volatizes the sample and excites the atoms. These processes take place simultaneously, influencing the resulting spectra-line intensities. The following excitation processes[1] determine the radiation output of the source for a given sample.

1. Processes that influence the entry of material into the excitation region - These include decomposition and volatilization of the sample.
2. Processes that control the transport of sample vapors through the source. These include diffusion, migration of ions in an electrical field, convection, transfer by a gas stream, and jets of sample vapor.

3. Processes that occur in the gaseous state (plasma processes). These include dissociation and formation of molecular species, ionization, excitation of free atoms and ions to higher energy levels by collisions and absorption, and radiative and nonradiative deexcitation of excited particles.

The excitation sources conventionally used for obtaining the line spectra of the chemical elements are the flame, the arc and the spark. Discharges at low pressure (glow, high-frequency, hollow-cathode and vacuum-spark discharges), radio-frequency torches, plasma jets and lasers are less commonly used sources. The principle difference between flames, arcs and sparks is the manner in which the excitation energy is supplied: by combustion in the flame and by an electrical current in the arc and spark. The temperature of the commonly used flames vary from 1700 to 3500°K and some flame temperatures are as high as 5000°K. The temperatures of normal low-current arcs range from 4000 to 7000°K. Spark temperatures are of the order of 10,000°K.

Vaporization and transport are assumed to give rise to a definite concentration (n) of the relevant chemical element in the gaseous state. If the particles are present in the gas as neutral atoms (n_a) and singly charged ions (n_i), the intensity of an atom line (J) depends largely on the proportions of the neutral and the singly ionized atoms, as shown in Figure 1. Therefore, in sources of sufficiently elevated temperature, such as arcs and sparks, ionization processes are crucial.

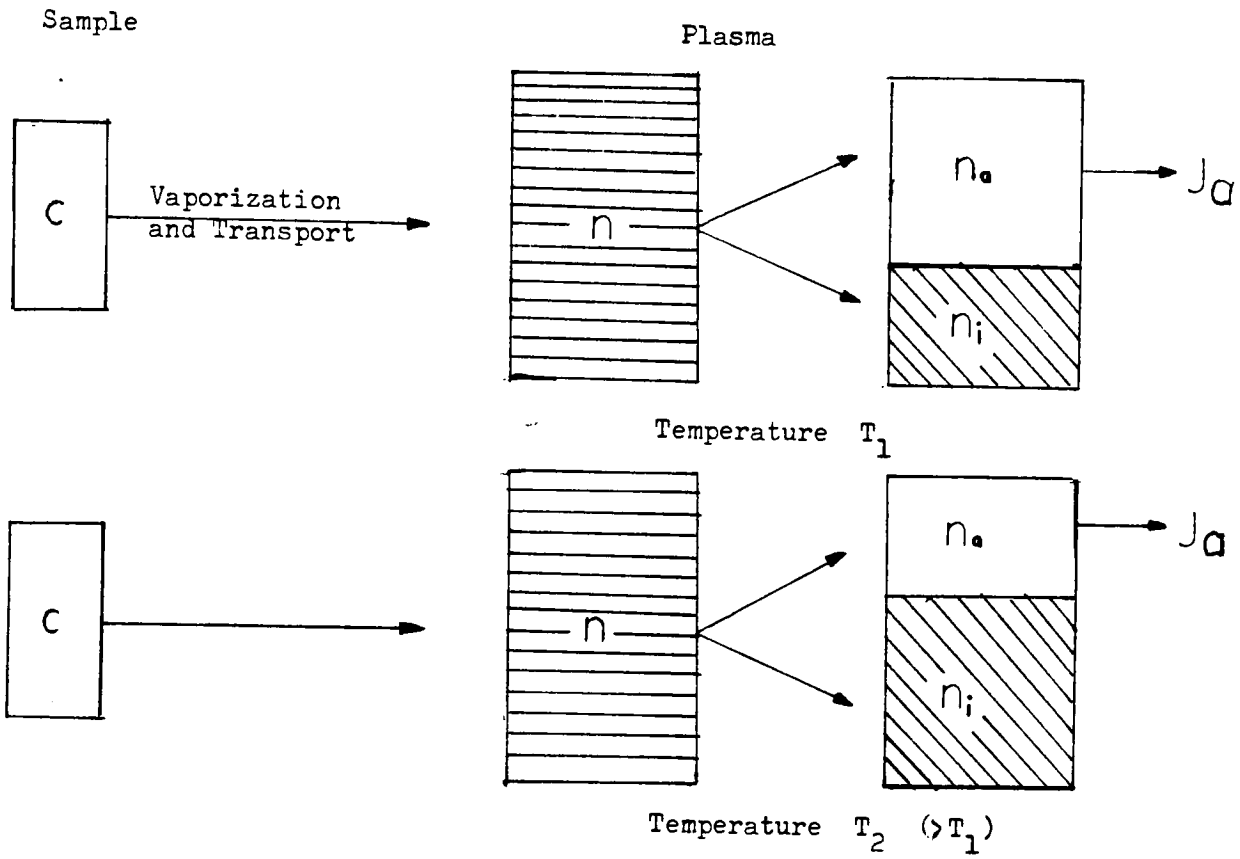

Figure 1
Schematic Illustration of the Significance of Ionization Equilibria for Spectral-Line Intensity (Ja)

Gases and vapors in the excitation region contain a partially ionized body. usually called a plasma. A plasma is a quasineutral gas of charged and neutral particles which exhibits collective behavior[2].

A plasma exhibits collective behavior because motions depend not only on local conditions but on the state of the plasma in remote

regions. Movement of charged particles generates local concentrations of positive or negative charge, which give rise to electric fields. Charges moving around also produce currents, and hence, magnetic fields. These fields affect the motion of charged particles far away.

Whenever local concentrations of charge arise or external potentials are introduced, they are shielded out in a short distance compared with the larger dimensions of the system. The bulk of the plasma is left free of large electric potentials or fields. The density of the ions and electrons are approximately equal and can be described by a common density called the plasma density. The plasma is quasineutral; that is, neutral enough, but not so neutral that all the interesting electromagnetic forces vanish.

The most vital parameter controlling the characteristics of a plasma is temperature. In general, the conditions of a plasma are characterized by different temperatures, each of which describes an aspect of the state of the system. For a monoatomic gas, four kinds of temperature exist:

1. The electron temperature, which is determined by the kinetic energy of the electrons.
2. The gas temperature, which is determined by the heavy particles (atoms, ions).

3. The excitation temperature, which describes the population of the various energy levels.
4. The ionization temperature, which governs ionization equilibria.

If all the temperatures have the same numerical value, a plasma is said to be in complete thermal equilibrium. This state is characterized by the following conditions:

1. The velocity distribution of all kinds of free particles (molecules, atoms, ions, and electrons) in all energy levels satisfies Maxwell's equation.
2. For each kind of particle, the relative population of energy levels conforms to Boltzmann's distribution law.
3. Ionization of each species is described by Saha's equation, while dissociation is described by the general equation for chemical equilibrium.
4. Radiation density is consistent with Planck's law.

A state of thermal equilibrium is established by collisions between material particles, emission and absorption of radiation, and chemical reactions. Complete thermal equilibrium prevails in an enclosure whose walls and interior have a uniform temperature with respect to radiation and internal energy.

The plasmas in analytical emission spectroscopy do not represent enclosed, adiabatic systems having uniform temperatures. There is always a net transport of energy and mass through the system and an inhomogenous temperature results. The condition in which thermal equilibrium prevails in separate volume elements of a nonuniform source is designated local thermal equilibrium (LTE).

High pressure plasmas are often characterized with a LTE plasma model. In LTE, the principle of microscopic reversibility is not completely fulfilled. The process of radiative emission (spontaneous and stimulated) are not balanced with radiative absorption processes, but because of the greater importance of collisional processes for obtaining the state of plasma equilibrium, the plasma is described as LTE[3]. In this model, chemical reactions which are nonequilibrium processes do not introduce considerable change in the equilibrium distribution of particles. For such a model, the relative concentrations of different species in the plasma can be calculated for any given temperature and pressure using the main principles of chemical kinetics.

If the conditions in the source change rapidly with time, different equilibria exist not only at different positions in space, but also at different times. This condition is typically called non-local thermal equilibrium (non-LTE). The non-LTE plasma is one in which

atomic and excited species exist in the plasma at temperatures lower than the electron temperature.

At lower pressures, the LTE approximation is no longer valid. Electrons gain energy in the field and transmit it to the heavy particles through collisions. Although the fractional energy loss in a collision is normally small, collisions of the highest energy electrons produce dissociation, ionization, excitation, and free radicals. These species are the reactants in neutral chemical chains operative in the plasma. Chemical reactions in non-LTE plasmas are described by considering individual reaction processes. It is necessary to know the energy distribution among the particles, time dependent distributions, the cross sections of the various reactions and thin energy dependence.

Many authors have reported non-LTE states in arc plasmas in inert gas and low current, less than 40 amps. An approximate non-LTE theoretical model of a two temperature plasma at high density has been developed assuming electrons take energy supplied by the electrical field[4]. This energy is partially transferred to atoms and ions by collisional processes. Figure 2 shows gas and electron temperatures calculated using this model and experimental measurements for an argon arc at two different currents (200 and 30 A). The results shown in Figure 2 agree with the experimental

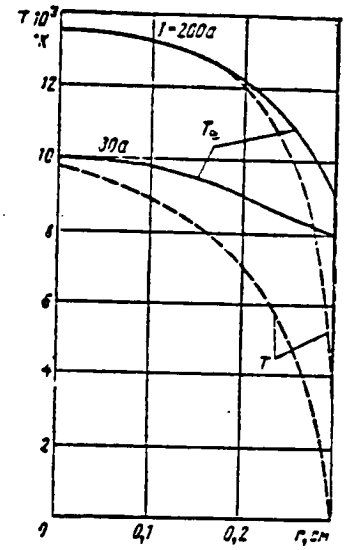

Figure 2
Radial Distribution T(r) Calculated for an Electric Arc in Argon According to Experimental Values of the Electron Temperature, $T_e(r)$

observations. Both theoretical and experimental results indicate non-LTE conditions are most likely to exist in a plasma with both low electron density and low concentration of molecular components.

Elements with high ionization potential will contribute less to the electron density of the plasma. The addition of such elements to a non-LTE plasma will not cause the establishment of LTE conditions.

The axial distribution of temperature in a vertical burning arc plasma mostly depends on the phenomena occurring near the cathode[5]. The surface of the electrodes and the very thin plasma layer immediately next to the electrodes are at lower temperatures than the plasma temperature. For arc plasmas with graphite electrodes, the temperature distribution along the axis is rather uniform. Approaching the cathode, the temperature increases by about 10%.

Dissociation, excitation, and ionization of particles greatly influence the plasma radial temperature distribution. Energy is transported mostly by heat conductivity in the radial direction of a vertical burning arc. Zones in which chemical reactions occur exhibit small radial temperature gradients relative to the arc plasma in general. The radial temperature distribution depends on all of the plasma components which exist in greater than trace concentrations.

The usual geometry for a low current arc in a magnetic field is described with the anode taking the form of a ring and the cathode as a rod in the center of the ring[6]. In a magnetic field, the plasma rotates around the edge of the anode forming a time-integrated picture of a rotating disk. This has several effects on the plasma, including:

1. increasing the residence time of particles in the plasma,
2. stabilizing the plasma,
3. better efficiency in introducing the sample into the plasma.

Ions and electrons rotate in the magnetic field and the neutral particles which are diffusing out of the plasma will be reintroduced several times by the plasma sector as it rotates. The overall effect is an increase in the residence time of particles in the plasma. Reflection is another factor causing an increase in the residence time of particles in the plasma. Particles colliding with the wall can either:

1. evaporate back into the plasma,
2. make refractory carbides on the wall,
3. diffuse through the wall.

The chemical nature of the sample species will determine the behavior.

The temperature distribution between the cathode and anode wall is the axial temperature distribution for a vertical burning arc. Because of this, the temperature distribution is rather uniform, as shown in Figure 3[7], with temperature differences about 13%. The distribution between the cathode and anode wall will depend on the ionization potential of an element.

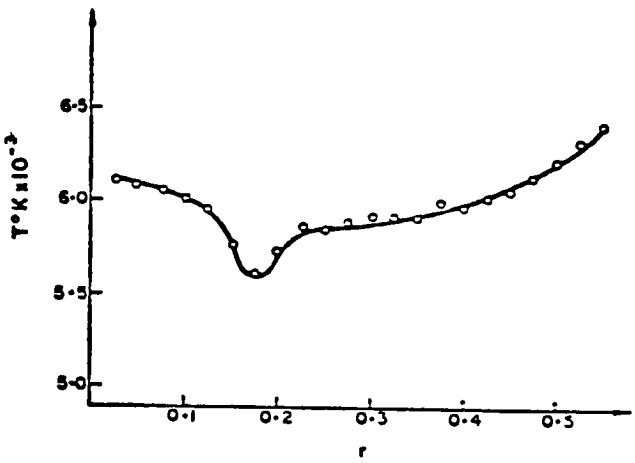

Figure 3
Radial Temperature Distribution in a Plasma
of a d.c. Arc Burning in an Inhomogeneous Field

The horizontal component of the magnetic induction is 4.6 x 10^{-3} T and the arc current is 10 A.

Zinc was chosen as the element for experiments because:

1. zinc has a high ionization potential (9.3 eV) and hence will contribute less to the electron density and thus cause the plasma to be more LTE;
2. the distribution between the cathode and the tube of an element with a high ionization potential is more homogenous relative to elements of low ionization potential;
3. zinc has low melting and boiling points and, therefore, atomic zinc will exist at low temperatures;

4. no data was found indicating zinc forms carbides and thus, zinc should be retained in the plasma for a longer duration compared to an element which forms a carbide with the tube;

5. zinc is nontoxic.

II. EXPERIMENTAL

A. Theoretical Calculations of the Concentrations of Different Species in an Equilibrium Plasma

In studying high temperature equilibria, the calculation of equilibrium compositions of complex systems becomes quite complicated and requires the use of of computers. A general computer program, called SOLGAS, for calculation of equilibrium compositions in systems containing an ideal gas phase and condensed phases of invariant stoichiometry was developed by Eriksson[8]. Appendix 1A describes the thermodynamic equations and the iterative procedure used by SOLGAS to calculate the equilibrium compositions.

SOLGAS, which is written in the FORTRAN language, was modified to be used interactively on the SIGMA 9. Data files were constructed according to Appendix 1B. The data from the JANAF Thermodynamic Tables[9] was read in and condensed by another FORTRAN program, PRESOL. The program used to run SOLGAS is described in Appendix 1C.

The JANAF Thermodynamic Tables included with the program did have data files for argon and complex carbon species, especially important for the system to be investigated.

Thermodynamic data was obtained for Zn(c), Zn(l), Zn(g), $Zn^+(g)$ and $Zn^-(g)$ from M. W. Chase, The Dow Chemical Company[10]. Other zinc species important to the system were $Zn_2(g)$ and ZnC(c), and no dissociation or spectroscopic information on which a thermochemical table could be based were obtainable. Ar, Ar^+, C^+ and C_2^+ thermodynamic data were found[11] and converted to units used in SOLGAS.

Calculations were done for two systems containing the following species:

Complex system - Zn(c), Zn(l), Zn(g), Zn^+, Ar, Ar^+, C (graphite), C(g), $C^+(g)$, $C_2(g)$, $C_2^+(g)$, $C_3(g)$, $C_4(g)$, $C_5(g)$, and electron gas

and

Simple system - Zn(c), Zn(l), Zn(g), Zn^+, Ar, C (graphite), C(g), and electron gas

The initial concentration chosen for each system was 96% argon, 2% carbon, and 2% zinc. The electron gas must be present for purposes of material balance. Calculations were done at temperatures from 400 to 6000K, approximately, every 200K and at one atmosphere pressure. Another series of calculations was carried out for temperatures between 300 and 800K every 50K where zinc is in equilibrium in all phases.

B. The Plasma Source

The source was fabricated to accommodate two rotating plasmas enclosed in a graphite tube serving as the anode in an external magnetic field. Due to the complexity of the system, the source was investigated using one rotating plasma illustrated in Figures 4 (a) and (b).

It was necessary to construct the source with optical access to the rotating plasma within the anode and still maintain a sealed cavity with the inert plasma support gas. Sapphire was chosen as the window material to enclose the hollow anode of the source. The useful qualities of sapphire are: nonconductivity, the ability to withstand temperatures in excess of 1100°C, and a particularly wide spectral transmittance. One of the windows was bored through the center to allow for the insertion of the cathode into the anode cavity.

The windows are held in place with housings connected to each end of the graphite anode. The housings are held in place with screws the length of the anode through the housings. The housings also support the gas flow inlet and outlet. They are constructed out of "Lava", a ceramic-like material capable of withstanding temperatures in excess of 1600°C. A good seal is maintained between the cathode rod and the sapphire window by a tiny lava fitting or sleeve.

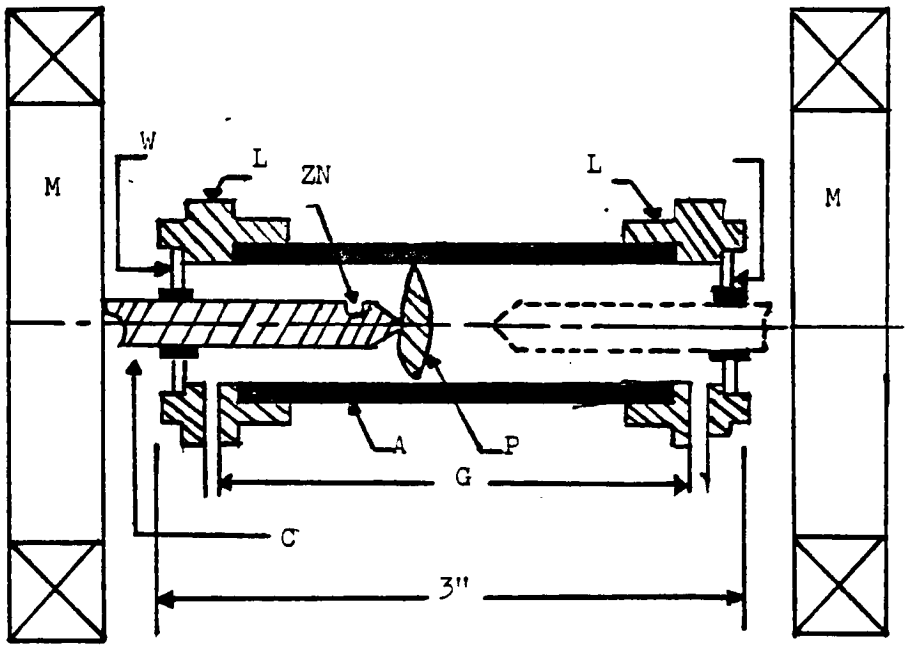

A - Anode
C - Cathode
G - Gas Inlets
L - Window and Gas Inlet Housing
M - Magnetic Field Coil
P - Plasma
W - Sapphire Window
ZN - Cavity for Zinc

Figure 4 (a)
Front View of the Low Current, High Pressure Plasma Chemical Source

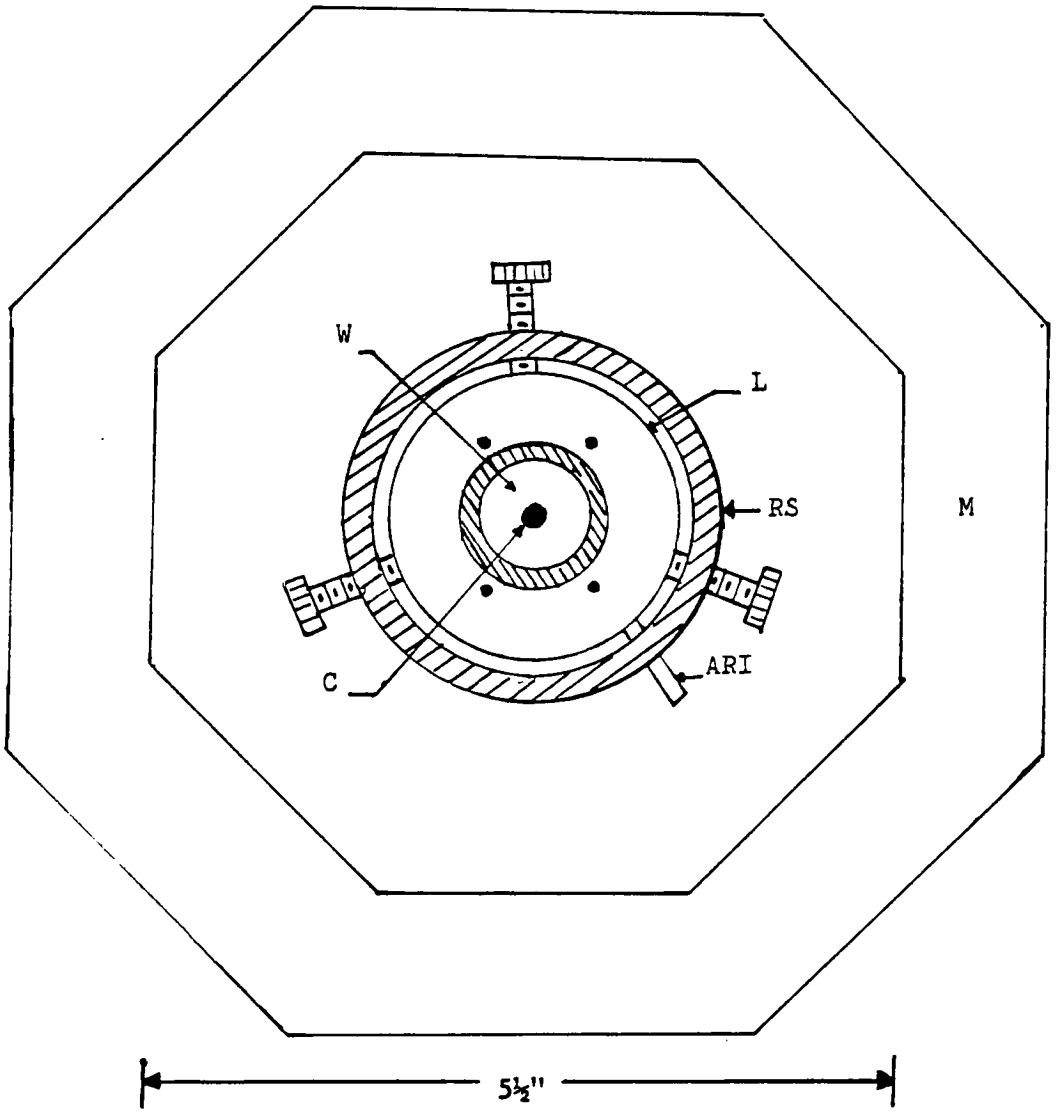

ARI - Argon Inlet
C - Cathode
L - Window and Gas Inlet Housing
RS - Ring Support
M - Magnetic Field Coils
W - Sapphire Windows

Figure 4 (b)
End View of the Low Current, High Pressure Plasma Chemical Source

The gas flow rate is measured with an in-line flow meter equipped with a regulator. With two meters connected in series into the inlet side of the anode, a maximum gas flow rate of 2.8 $\pm$ 0.1 liters $\bullet$ minute^{-1} at STP can be achieved. The meters were calibrated via the displacement of water in a unit of time. A commercial in-line gas purifier was utilized with capabilities of reducing the amounts of oxygen and water normally found to below 1 ppm.

Two Helmholtz coils were wound on aluminum forms and mounted equidistant from the axial center of the plasma source. Each coil was wound with approximately 1000 turns of 18 gauge magnet wire. The resistive load of each coil was subsequently balanced to 12 ohms. The coil set was operated in series with a 1000 watt DC power supply to provide a maximum field strength of 225 gauss. The uniformity of the radial component of the magnetic field was determined[12] to be less than 7 gauss under all conditions investigated. The variation in axial field strength through a rectangular volume of 2 cm x 2 cm x 4 cm located at the midpoint between the coil set was less than 3% at 164 gauss. The magnetic coils were cooled during use by circulating water through tubing wound around the aluminum forms.

The arc is maintained with a Jarrell Ash constant current 160 volt DC power supply, variable from 2.5 to 15 A. The arc is started by a built-in tesla-coil igniter.

C. Introduction of Zinc into the Plasma Source

The cathodes were made from carbon rods purchased from Bay Carbon, Inc. of Type 3/16 x 6 inches (Lot No. 080281). The rods were broken in half and one end was sharpened with a small hand-held pencil sharpener. The point on the cathode provides a high concentration of electrons when the source is struck for the arc to ignite. Approximately 13/32 inch from the tip of the cathode, a hole 5/32 inch deep was drilled with a 1/16 inch drill bit.

The cavity of the cathode was packed with 15 mg of 'Baker Analyzed' 20 mesh granular zinc (Lot No. 846401). A mark was made on the carbon rod to ensure the tip would be centered in the magnetic field and source. Precautions were taken not to deposit impurities onto the cathode during fabrication. The cathode tip and anode tube will heat after the ignition of the arc. During the arc burning, zinc evaporates into the plasma.

D. Qualitative Investigations of the Source

The optical access of the source was placed on an optical bench which was aligned with a λ-Minuteman polychrometer using a helium-neon laser. The image of the source was projected onto a slit placed on the optical bench. A 1 mm slice of radiation between the cathode and anode wall was cut and focused onto the

entrance slit of the polychrometer as shown in Figure 5. The entrance and exit slits were 20 mu.

The polychrometer was a modified Czerny-Turner system with a reciprocal linear dispersion of approximately 8 Å/mm. The polychrometer was equipped with a 1200 line/mm grating blazed at 5000 Å. The focused radiation was detected by a photomultiplier tube (PMT) placed at the center of the exit slit holder. The PMT was a red sensitive Be/Cu with S-1 spectral response. The high voltage for the PMT was 500 V.

The signal from the photomultiplier tube could be displaced on a storage oscilloscope (Tektronic, Inc. Type 561 B). A permanent record was obtained by photographing the time resolved event on the oscilloscope screen. A 35 mm camera equipped with a 50 mm lens on a tripod was used.

A spectrum was obtained by either channeling the signal through a picoammeter to a chart recorder or directing the throughput of the signal onto spectrochemical film or plates. For film or plate usage, the PMT housing unit must be removed and the appropriate holder put in place.

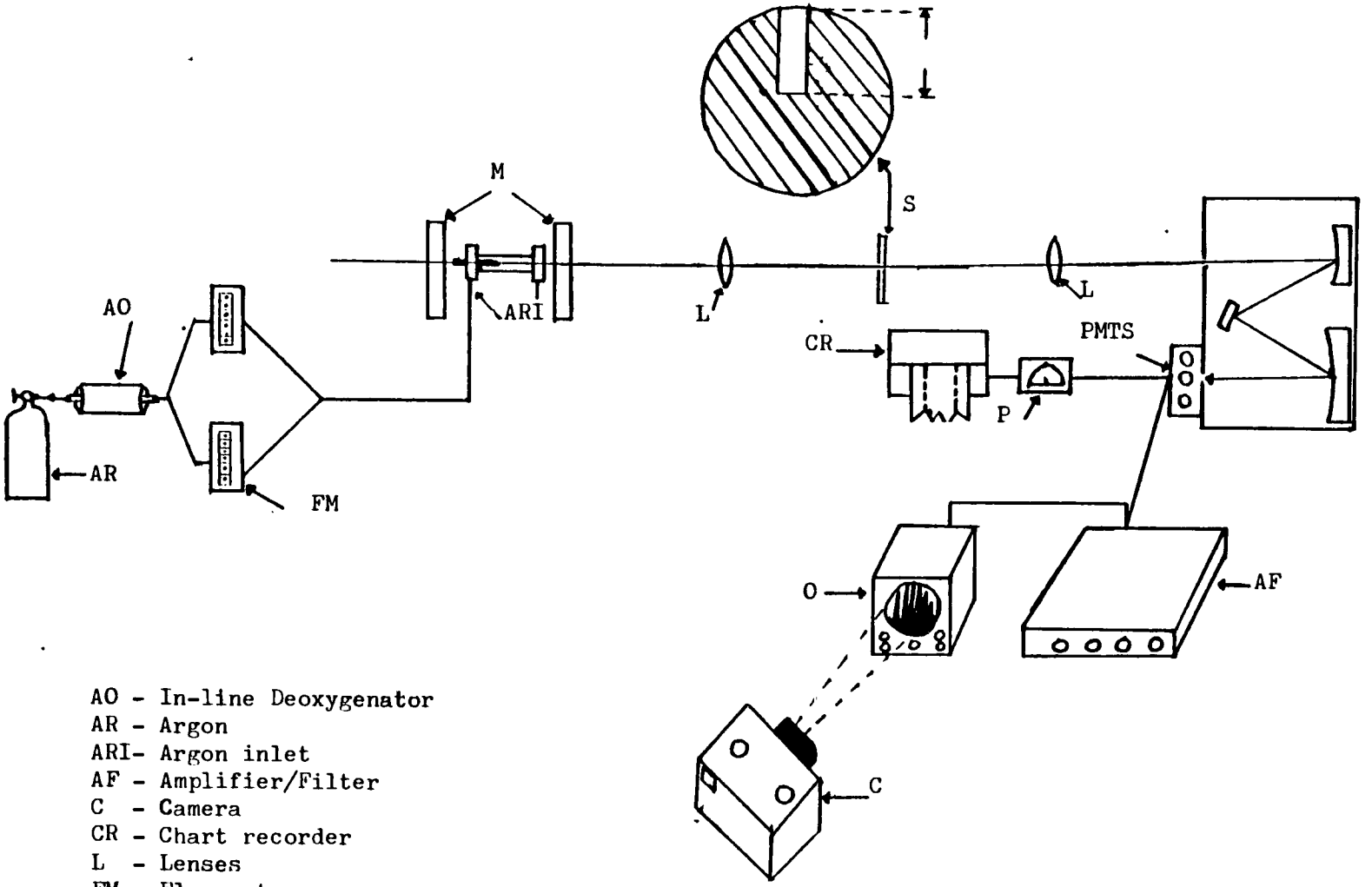

AO - In-line Deoxygenator
AR - Argon
ARI- Argon inlet
AF - Amplifier/Filter
C - Camera
CR - Chart recorder
L - Lenses
FM - Flow meters
M - Magnetic Field Coils
P - Picoammeter
O - Oscilloscope
S - Slit

Figure 5. Optical alignment of the plasma chemical source.

The source was operated at a 3 A arc current, 83 G magnetic field, an argon flow rate of 1.4 liters/minute (STP), and a 15 mg sample of zinc for the qualitative investigations, unless indicated otherwise.

1. Spectra of the Arc Source

   a. Argon Plasma

      The argon spectrum was obtained from 4000 to 3000 Å (Figure 6) and spectral lines were assigned[13] for the region between the cathode and anode wall with a chart recorder using the following specific settings.

      1. Chart speed - 1000 Å/inch
      2. Rise time - 3 seconds
      3. Picoammeter - 10×10^{-19} A
      4. Argon flow rate - 2.8 liters/minute

   b. Argon/Zinc Plasma

      The zinc/argon spectrum is shown on photographic film from 4500 to 3000 Å in Figure 7 (a). Also, shown in Figure 7 (b) is the spectrum of a low pressure mercury source. The zinc and mercury spectral-lines were assigned[14].

2. Time Dependence of Zinc Concentration and Frequency of Rotation

   The storage oscilloscope was used for the determinations of the dependence of zinc concentration and frequency of

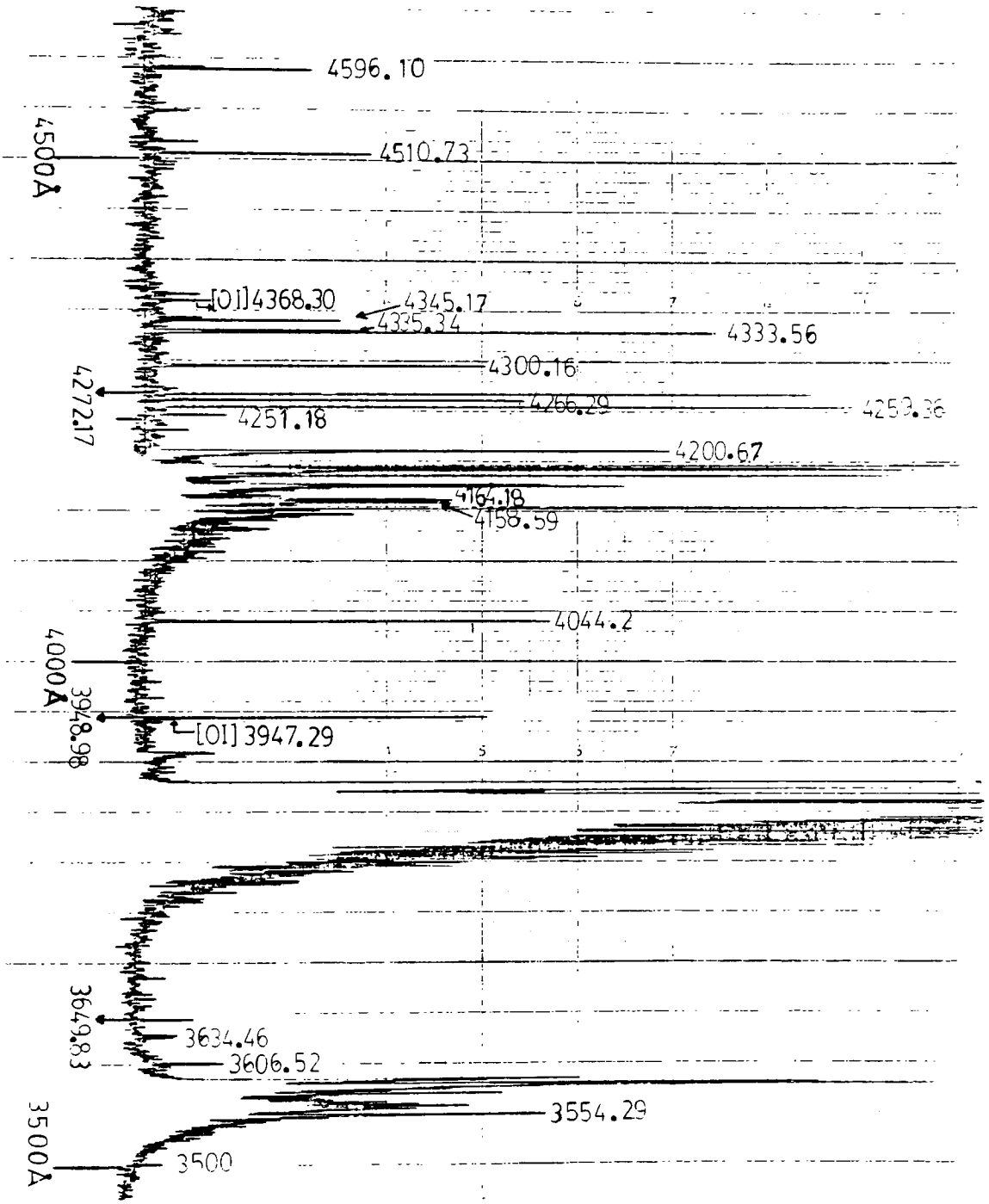

Emission Spectrum of an Argon Plasma

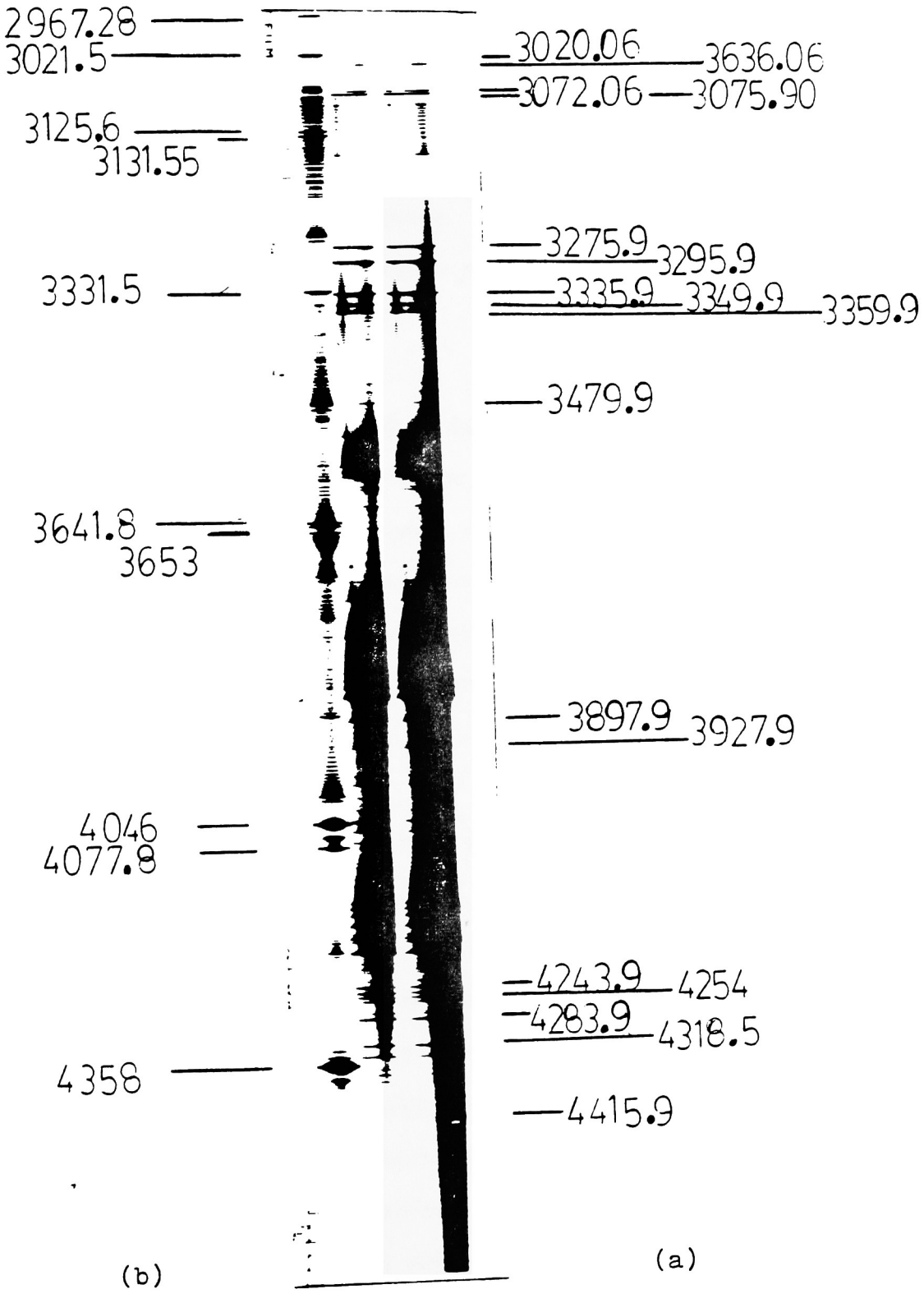

Figure 7
Emission Spectra of (a) the Source with an Argon/Zinc Plasma, (b) a Low Pressure Mercury Source

rotation on time. A typical photograph of 3076 Å zinc atomic line is shown in Figure 8. Each peak represents one arc rotation, with a 20 msec/div time scale approximately 16 rotations are observed. The intensity scale was set at 1 V/div. Data was taken every minute for 10 minutes, after igniting the arc.

3. Gas Temperature of an Argon/Zinc Plasma

A W/Rh thermocouple was placed slightly off center and 1/2 inch from the plasma. A lava sleeve held the thermocouple in place and maintained a good seal. Voltage readings were obtained during a 14-minute period after igniting the arc. Temperatures were extrapolated from the thermocouple calibration curve (mV vs. temperature)[15].

E. Determining Temperature Using Photographic Film

1. Photographic Detection

Photographic emulsion is a sensitive detector that is widely used in emission spectrometry. It actually serves as a composite detector-transducer-amplifier-recorder and provides a permanent record of the intensity and spatial pattern of the incident radiation. An emulsion consists of minute silver halide crystals dispersed on a transparent, water-expandable medium such as gelatin on film.

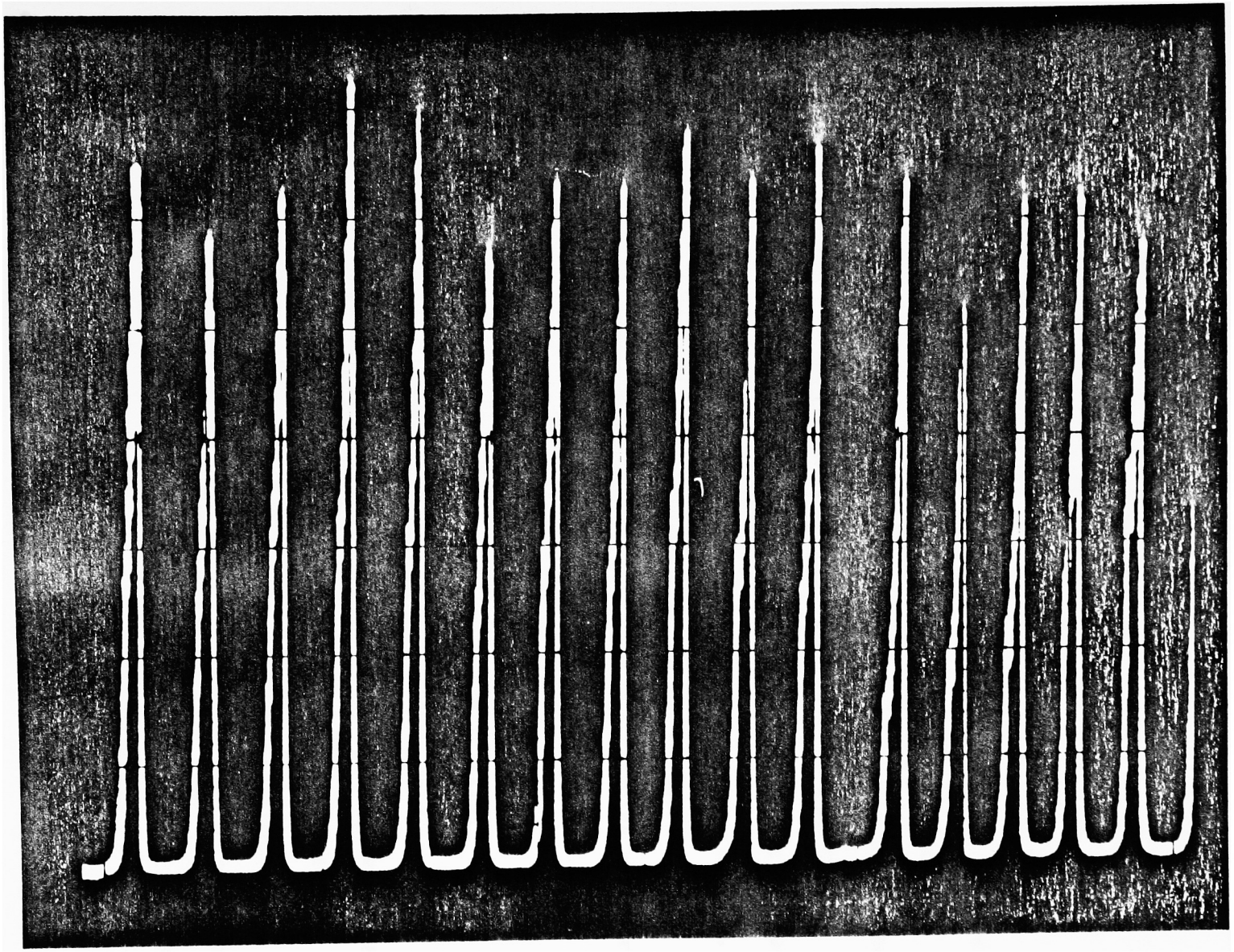

Figure 8. Photograph of a storage oscilliscope screen to determine the average intensity between the cathode and anode wall and the frequency of rotation of the Zn 3076 Å spectral line.

On exposure, the silver halide crystals receiving radiation build a latent image. Subsequent chemical development, which is analogous to amplification, produces a black deposit of silver at the site of the latent image. Emulsions give high spatial resolution since their silver halide crystals are small. After development, the emulsion must be fixed in a solution which dissolves the unexposed silver halides. Finally, the photographic material must be washed thoroughly to remove the chemicals used in the developing and fixing. The entire series of operations must follow rigidly controlled conditions with respect to time, temperature, and chemicals. The density of deposit is ordinarily determined by a photoelectric scanning procedure.

a. The Film

Kodak spectrum analysis Film Number 1 (0667), (Lot No. 0-667-001-131) was used. The film is characterized by low speed, fine granularity, very high resolving power, and high contrast[16]. The latter two characteristics, plus low background, make this film especially suitable for trace element work in the region from 250 to 440 nm, where a weak spectral line must be distinguished from background radiation.

b. Film Processing

The exposed pieces of 35 mm film were placed on a piece of plexiglass equipped with metal clips to hold the film in place. Holes were drilled through the holder, aiding in the agitation of the solutions and holding the film in place when solutions were changed.

The film was placed in Kodak Developer D-19 for 5 minutes with continuous agitation at 20°C. Subsequently, the film was rinsed for 30 seconds with water and then placed in Kodak Fixer for 10 minutes at 20°C with frequent agitation. The final processing step was to wash the film in running water for 20 minutes and dry. The solutions were prepared according to the manufacturer's directions and changed for each batch of film developed.

c. Measurement of Density

The comparison of line intensities on a photographic film requires the use of an instrument that will measure the relative transmittance of the line images. Figure 9 shows a schematic diagram of such a device, a simple microphotometer[17]. As the instrument scans a spectrum, the amount of light from a tungsten lamp impinging on the detector will change, and different

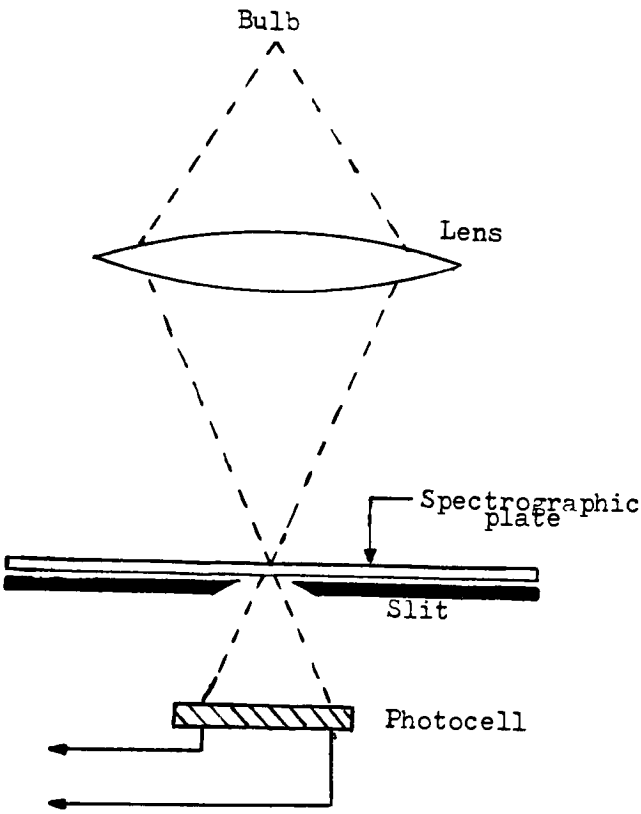

Figure 9
Schematic Diagram of a Simple Microphotometer

currents will result. These are presented with a pen record on a chart. Many commercial microphotometers operate somewhat differently, using a projection technique allowing direct readout of density determinations. Generally, they are referred to as densitometers.

The instrument used was an ANSCO Automatic Recording Micro- densitometer, Model 4. An aperature size of 0.5 mm and an eye objective of 10/5 were used.

2. Calibration of the Film

The response of a photographic material varies with the spectral distribution of the exposing light or other radiation. Therefore, the radiation used to expose the material in sensitometric tests must simulate that to which the material is normally exposed in practice. For this, a 3 x 5 inch piece of glass was coated with Eastman White Reflective Paint and placed in front of the slit on the optical bench. An Eppley Laboratory continuum source calibrated over the range of 250-1600 nm in terms of the 1973 NBS Spectral Irradiance scale was placed behind the slit and next to the polychrometer. The method afforded a uniformly lit slit. Exposure times were varied from 10 seconds to 3 hours with the source operated at 7.90 amperes DC.

Each plate was exposed to the plasma source containing zinc so that wavelengths of interest could be found after development. Measurement of the various densities in the processed sensitometric strip, when plotted against the exposures from which they were derived, produce a characteristic curve[18] similar to that shown in Figure 10.

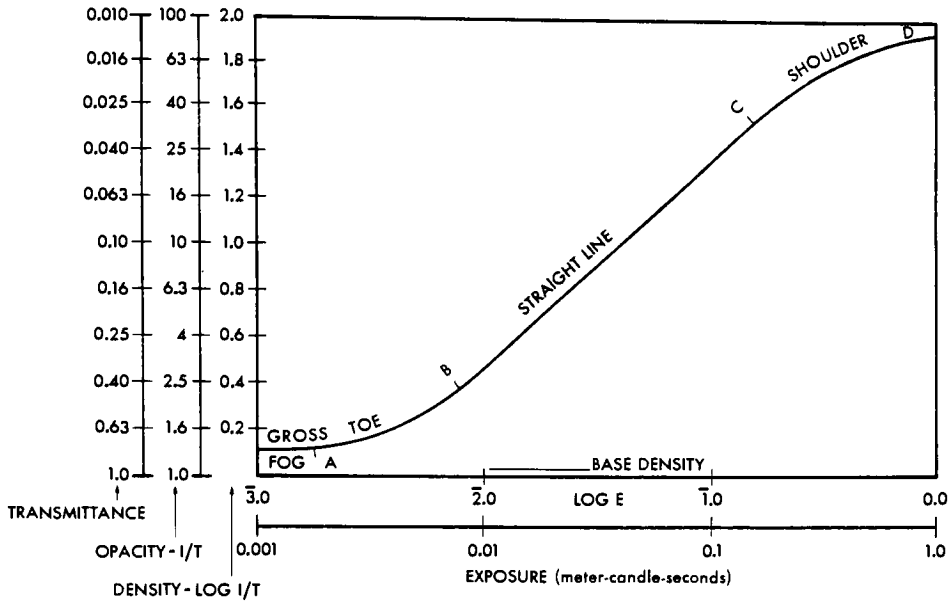

Figure 10
Characteristic Curve Representative of a
Negative Photographic Material

The characteristic curve, usually a plot of density vs. logarithm of exposure, demonstrates the way in which a plate or film responds to exposure and development. The slope at any part of the curve indicates how rapidly the density changes with changes in exposure.

In the midsection of the characteristic curve (B to C), density shows a linear relationship with the logarithm of the exposure. Some plates and films have a long straight-line portion, whereas others have little or none.

In quantitative photographic work, the best results in terms of precision and accuracy will be achieved when optical densities are in the linear region of the characteristic curve. Exposure differences do not change significantly with density differences in the toe (A to C) and shoulder (C to D) regions.

Densities can be correlated to a series of isointensity exposures of known exposure time in the same manner. Such a calibration is called a time-scale calibration, and the curve a density-log time characteristic curve. It has been shown[19] the density-log time characteristic curve is identical with the density-log intensity characteristic curve for most spectrochemical emulsions.

3. Method of Temperature Determinations

Temperature measurements using an atom-atom pair of lines have been described[20]. The difference in the intensity of two atom lines of the same element in a source will depend upon the statistical weights, frequencies, transition probabilities, and the excitation energies. If these are defined for a pair of atom lines, the absolute temperature can be determined using the Maxwell-Boltzmann distribution law. It is desirable for the energies to be significantly

different. In addition, it is desirable to have a pair of atom lines close together when using photographic detection. This would eliminate the necessity of calibrating the film for two completely unique wavelengths. The Zn 3076/3072 Å atom-atom line pair satisfy the criteria.

4. Source Parameters and Intensity Determinations

The intensities of the atom-atom line pair were determined varying the following parameters.

1. Magnetic field
2. Arc current
3. Argon flow rate
4. Amount of zinc sample

The exposure times necessary to obtain atomic line intensities within the linear region of the calibration curve varied from 10 to 30 seconds. Three different exposure times were made for each condition between the cathode and anode on a single plate by adjusting the height of the film holder. The film was processed and the optical densities of the atomic zinc lines were measured by scanning from 3070 A to 3078 Å. The distribution of zinc between the cathode and anode was obtained from 6 to 12 cross-sectional scans. The intensity was determined by the extrapolation of

the observed optical density from the obtained characteristic curve for the film. In some cases, the line intensity needed to be corrected for the spectral background. The method consists of converting densities into intensities, not log intensities, and subtracting the background intensity from the line-plus-background intensity. As a rule[21], background densities of the order of 0.10 may be ignored, especially if the background underlying both lines is essentially constant.

F. Investigation of the Argon Plasma

1. Spectroscopic

An LSI-11 microcomputer was interfaced to the polychrometer for the collection of spectral data. The polychrometer was configured as shown in Figure 5 to observe several Ar emission lines simultaneously. Data acquisition programs were written by G. Fazekas[22]. Computer programs were written in BASIC to set up files and reduce and store data, Appendix II.

a. Argon Spectral Lines

From the spectrum of the Ar plasma, Figure 6, three lines were chosen for quantitative work. One of these lines, 3948.98 Å was selected because it was well separated from disturbing spectral lines. A spectral line at 4272.17 Å was used because of the intensity.

The third line, 3649.83 Å was selected because its energy of transition was high. In choosing these lines, other considerations were: the spectral width of the polychrometer was 1300 Å, and the lines were spaced out allowing easier PMT alignment.

b. PMT Calibration

PMT's will respond differently to incident radiation. These differences were compensated for by measuring outputs from a frequency generator input of 400 Hz. Source emission intensities were corrected for these differences.

c. Determination of Argon Emission Intensity

The data acquisition programs allowed the number of channels to be used, the number of data points to be collected, and the rate of sampling to be specified. Usually a data point was obtained approximately every 150 microseconds for 1/60 for a second for each channel. The sampling rate allows reproduction of the plasma source rotation on a storage oscilloscope screen. Subsequently, the emission intensities as voltage counts could be stored on disk. A BASIC program was used to determine the maximum intensity at each rotation. Usually, a minimum of 20 rotations were averaged to determine the spectral line intensity.

d. Background Correction

Corrections for background radiation from the source itself must be made. The method[23] used involved measuring the total intensity at the wavelength of the line. The wavelength setting was changed 2 Å, and the adjacent background contribution from the source was measured on both sides of the line, in the same manner as the line intensity. The average of the readings was subtracted from the total intensity.

e. Radial Distribution of Argon

The radial distribution of an argon plasma was determined by masking different regions of the source between the cathode and anode. A reproduction of stored intensities of each argon line along with the associated background radiation is shown in Figures 11 (a), (b) and (c). A peak maximum is obtained when the arc passes in front of the slit. The intensities shown represent a 1 square millimeter from 2 millimeters above the cathode. The source parameters were: magnetic field current of 83 G, source current of 4 A, and an argon flow rate of 2.6 liters/minute.

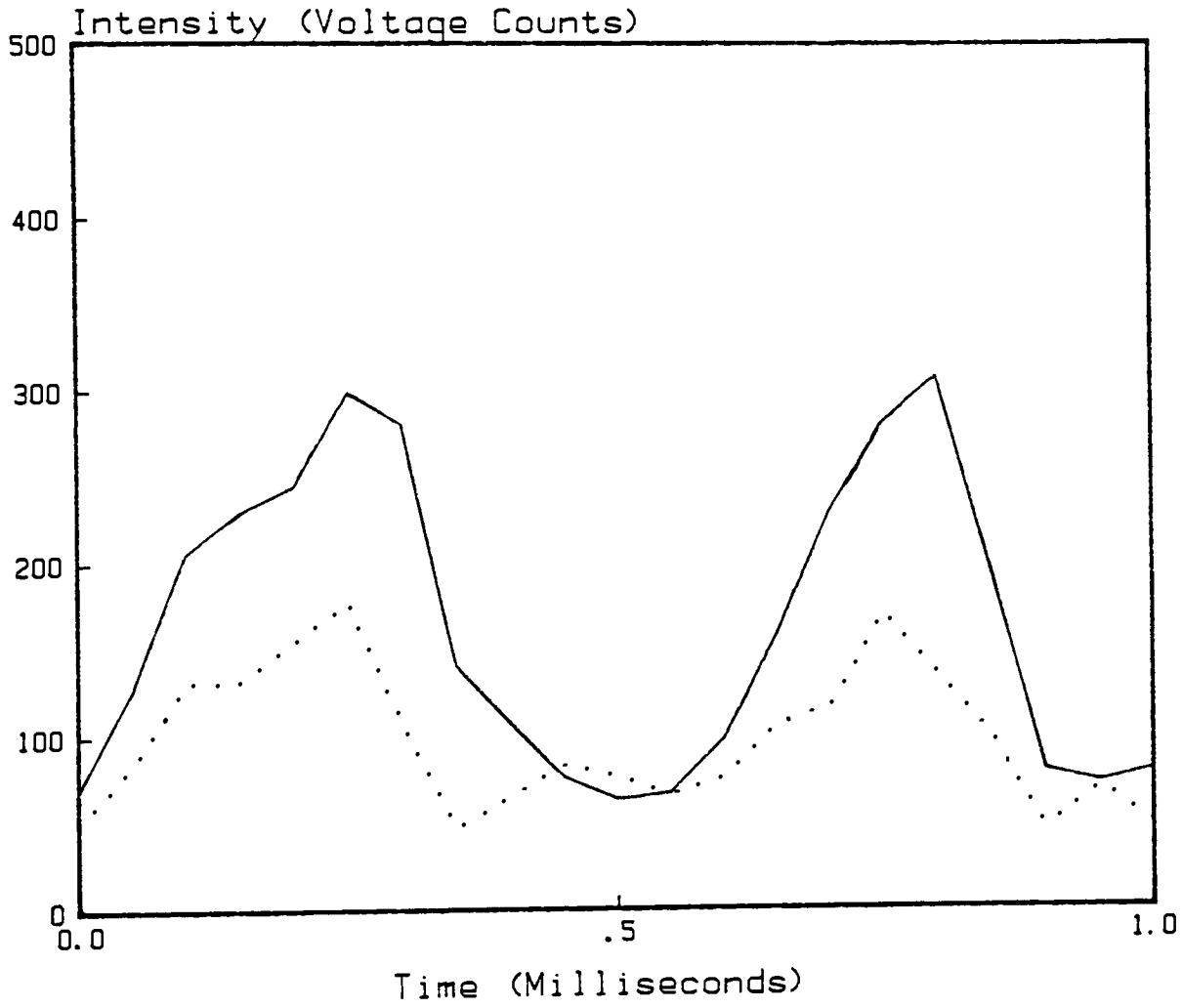

Figure 11 (a)
Emission Intensity of an Argon(-) Plasma and Associated Background Noise (•) at 3649.83 A With Time

Distance from the Cathode - 2 mm
Optical Access - 1 square mm

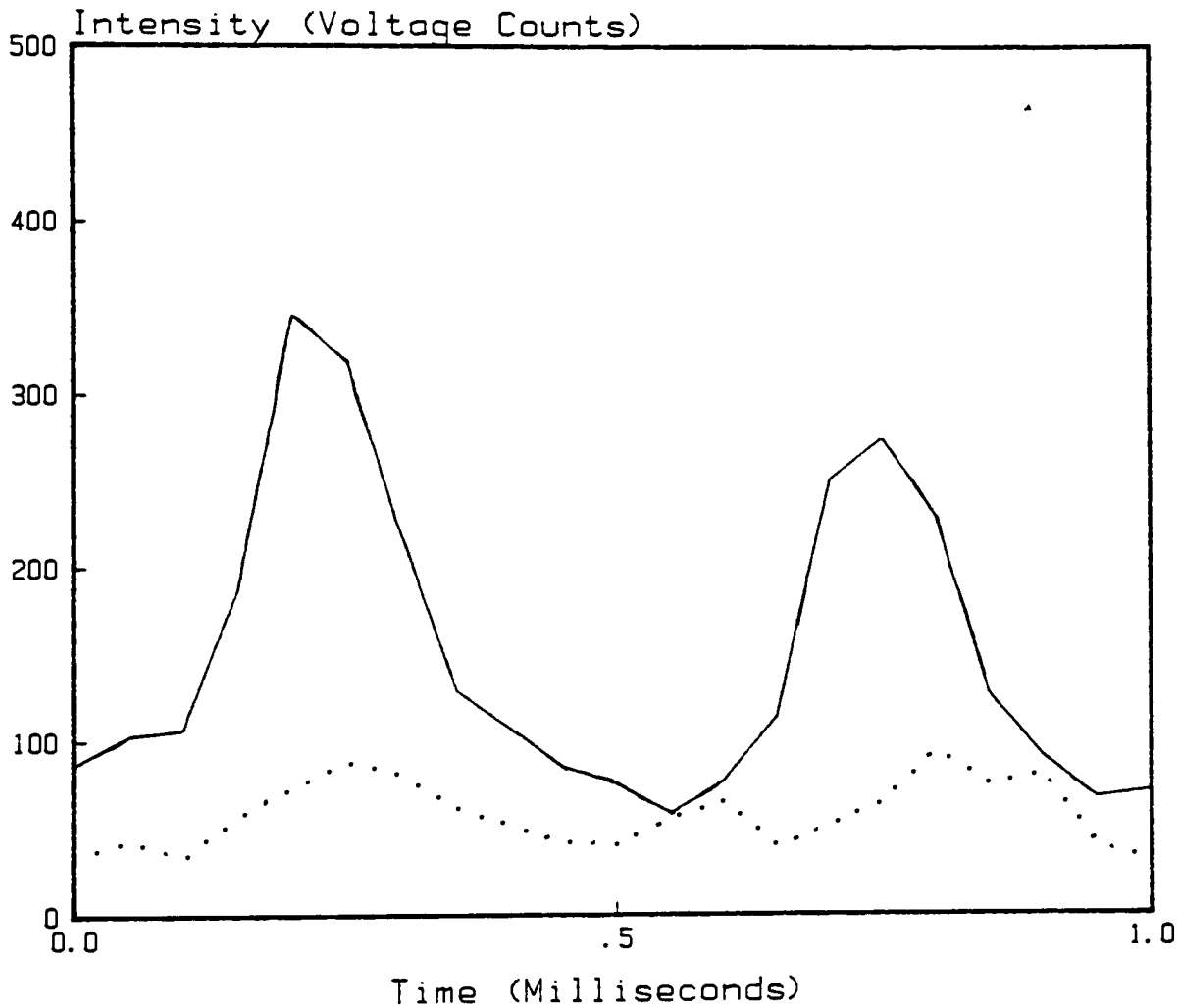

Figure 11 (b)
Emission Intensity of an Argon(-) Plasma and Associated Background Noise (•) at 3948.98 A With Time

Distance from the Cathode - 2 mm
Optical Access - 1 square mm

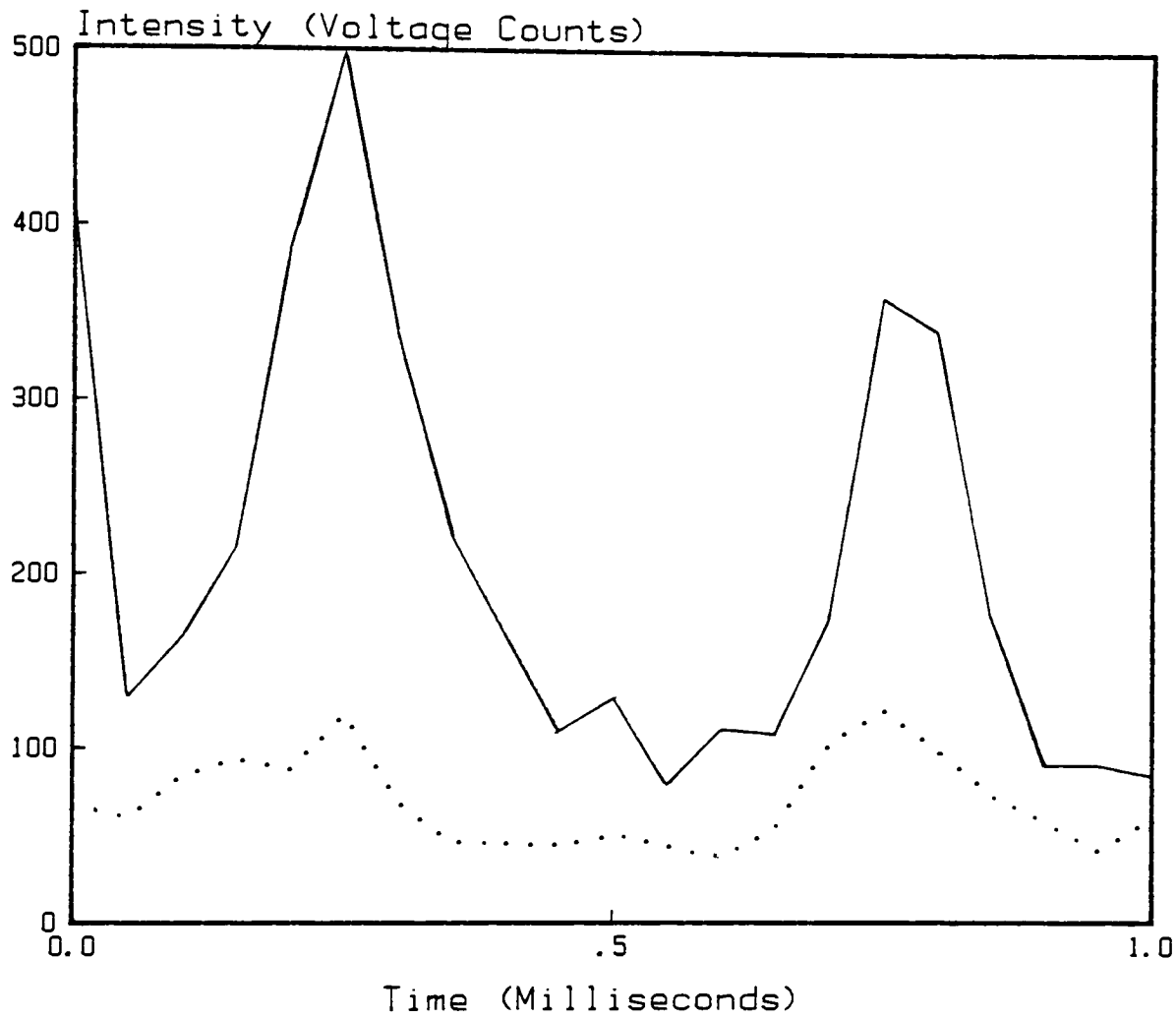

Figure 11 (c)
Emission Intensity of an Argon(-) Plasma and Associated Background Noise (•) at 4272.17 A With Time

Distance from the Cathode - 2 mm
Optical Access - 1 square mm

The radial distribution, using the same conditions, with argon spectral-lines, was unobtainable in an argon/zinc plasma. The background radiation for the 3649.83 Å line was equal to the measured intensity of the line. The background radiation at 4272.17 Å, the most intense argon line, accounted for 75% of the total line intensity. However, an average distribution of radiation was obtained by measuring the intensities from the whole region between the cathode and anode.

2. Temperature of Gases in an Argon Plasma

Gas temperatures were measured using an iron-constantan thermocouple that was 0.076 inches in diameter as a function of time, up to approximately 14 minutes. Temperatures were determined for several different distances between the thermocouple and cathode tip. Pertinent source parameters were: an argon flow rate of 1.4 liters/minute, a magnetic field current of 83 G for arc currents of 3 and 4 A.

III. RESULTS

A. Computer Calculations of the Concentration of Different Species in an Equilibrium Plasma

Equilibrium calculations for the argon, zinc, and carbon systems were computed as mole fractions and plotted versus temperature in Figures 12, 13 and 14.

The total mole fraction of species contributing ions at 5400 K can be determined from Figure 12 to be approximately 1.0×10^{-10}. Various carbon species are prevalent at temperatures greater than 3600 K, due to the sublimation of carbon. Contributions from ions and various carbon species at equilibrium are small even at high temperatures, as shown by comparing Figures 12 and 13.

Another series of calculations (Figure 14) was carried out for temperatures between 300 and 800 K where zinc is in equilibrium in all phases. Temperatures in excess of 600 K are necessary for the presence of a significant amount of gaseous zinc.

Figure 12. DISTRIBUTION OF SPECIES IN THERMAL EQUILIBRIUM (COMPLEX SYSTEM)

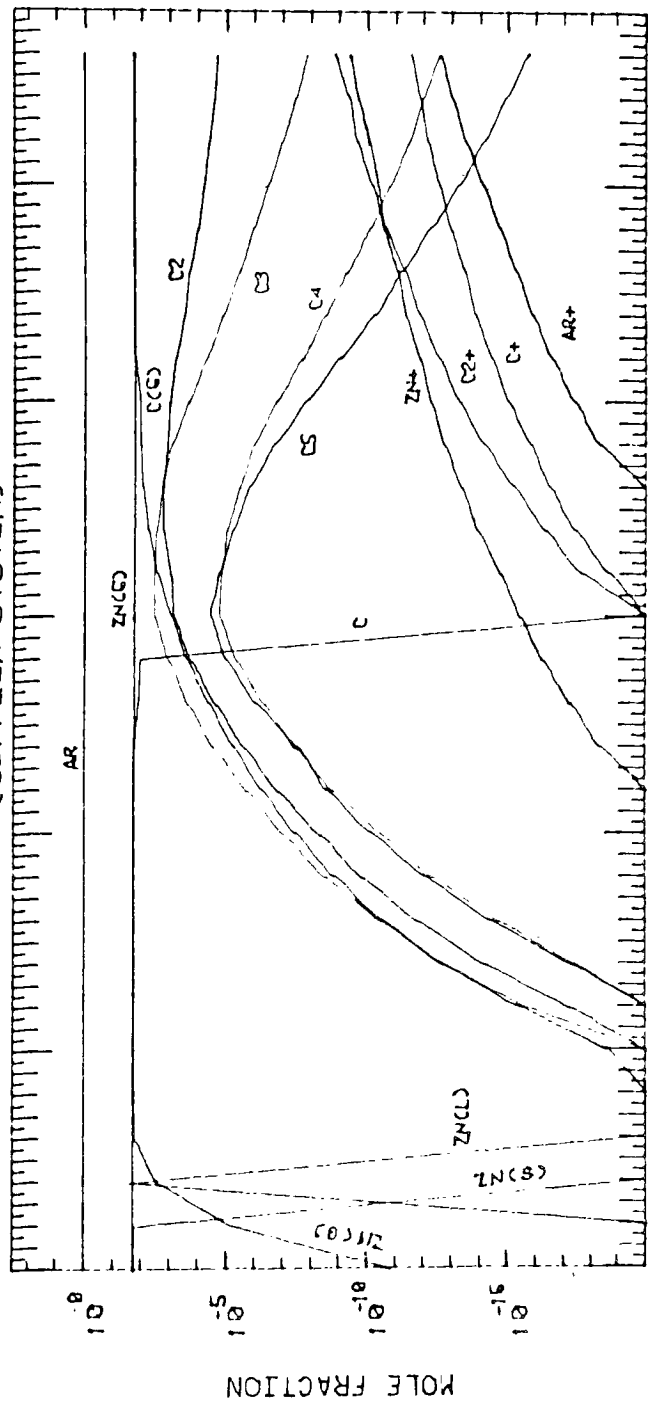

Figure 13. DISTRIBUTION OF SPECIES IN THERMAL EQUILIBRIUM (SIMPLE SYSTEM)

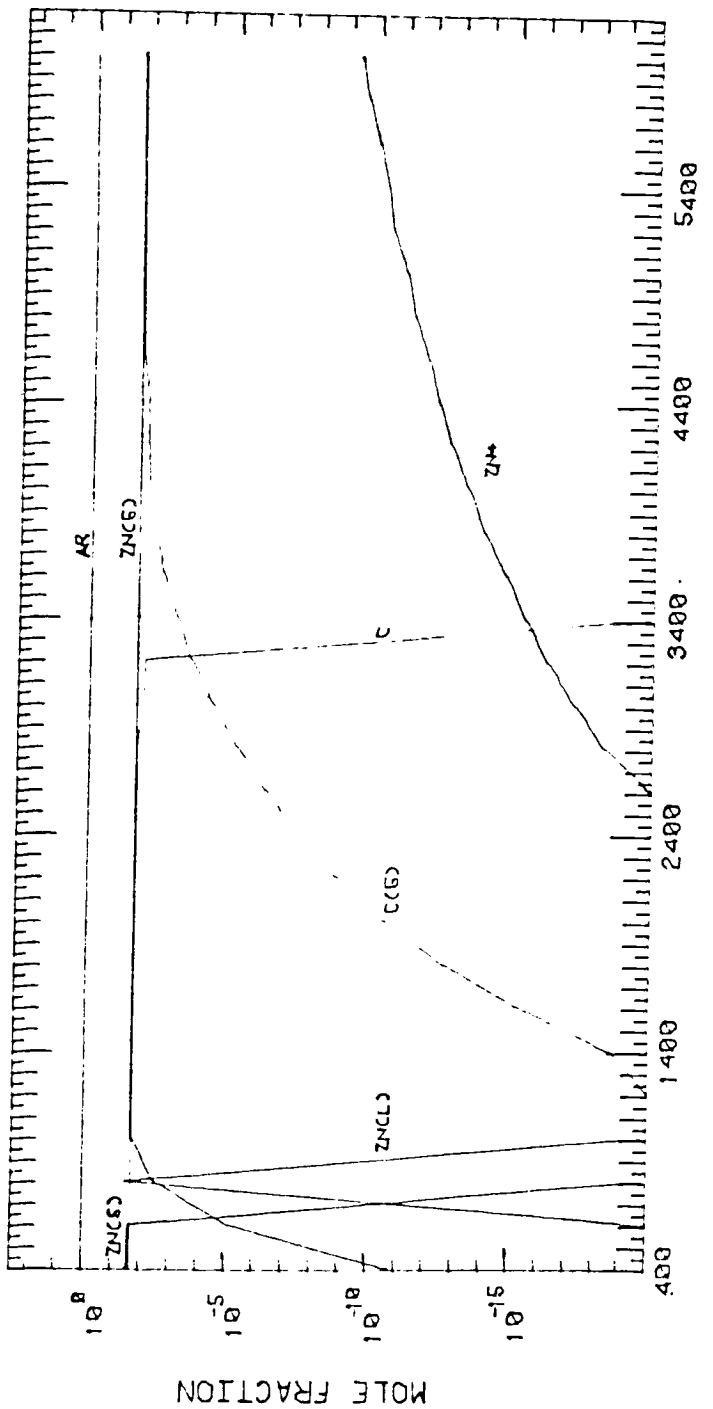

Figure 14. DISTRIBUTION OF SPECIES AT LOWER TEMPERATURES IN THERMAL EQUILIBRIUM

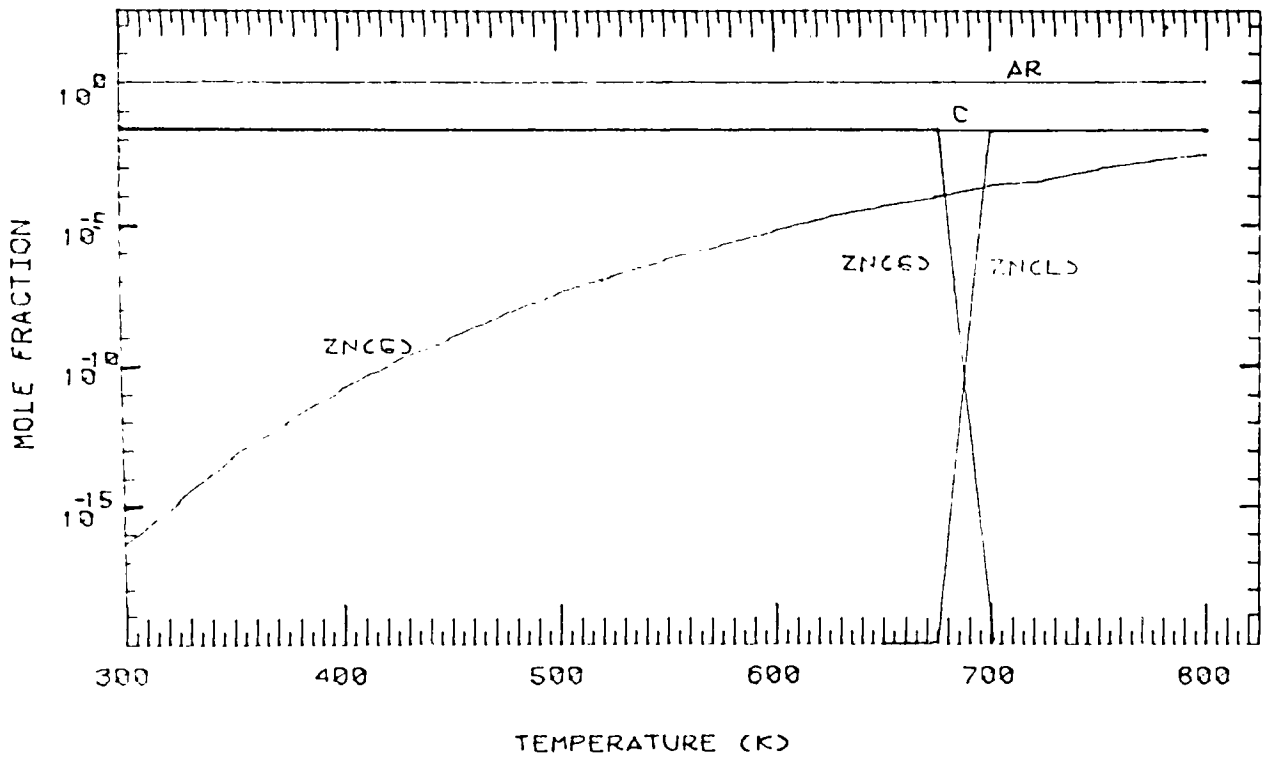

B. Impurities in the Plasma

1. Argon Plasma

Two oxygen lines, 3947.29 and 4368.30 Å, are documented[24] for the region of the spectrum shown in Figure 6. The spectral lines were weak and only the longer wavelength line was resolved from argon emission. Emission from atomic nitrogen was not found.

Two weak molecular bands were observed in the regions 3520 to 3590 Å and 4100-4200 Å. A strong band emission was found between 3750 and 3880 Å. These are probably cyanogen molecular bands.

Oxygen and nitrogen are impurities in common argon gas supplies due to the close melting and boiling points of the elements[25]. When an arc is operated between carbon electrodes in the presence of nitrogen, some cyanogen (CN) molecules forms and, being excited by the arc, emits typical molecular band spectra in the region from 3600 to 4200 Å[26]. Molecular spectra are intense, complex, and obscure regions of the ultraviolet useful in atomic emission spectroscopy. High purity argon gas containing small amounts of impurities, less than 1%, is available, but it is very expensive. Molecular band emission should diminish with the use of high quality argon in this source, since the arc is operated in a closed chamber with a flowing stream of argon.

2. Argon/Zinc Plasma

When solids are heated to incandescence, continuous radiation is emitted that is more characteristic of the temperature of the emitting surface than of the material of which it is composed. The radiation is produced by the innumerable atomic and molecular oscillations excited in the condensed solid by the thermal energy. The continuous background radiation could also be emitted by the heated cathode of the arc as shown in Figure 7. The background radiation diminishes at shorter wavelengths where very high temperatures are needed for a substantial amount of thermal excitation at atmospheric pressure.

The most intense and resolved argon spectral lines were discernable in the argon/zinc plasma. The argon spectral lines chosen for temperature analysis were 4272.17, 3948.98 and 3649.83 Å. The spectral lines at 3649.83 and 3948.98 Å have large excitation potentials and were not observed. The argon line at 4272.17 Å is hazy and partially obscured by the molecular band and the continuous radiation.

Iron and lead are impurities, approximately 0.002%, in the granular zinc. The most intense emission lines were not found for either element.

The zinc emission lines used in temperature studies, 3075.90 and 3072.06 Å, are resolved with little spectral interference. The intensity of zinc emission at 3072 Å was found to be weaker than at 3076 Å, corresponding to a higher energy of excitation. These intensity differences make photographic detection of both spectral lines difficult for a variety of source conditions.

C. Achievement of Steady State

1. Time Dependence of Zinc Concentration and Frequency of Rotation

After the arc is turned on, the intensity of the Zn I 3076 Å line increases and the frequency of rotation decreases, Figure 15. The intensity of a spectral line is not only a function of the atomic concentration. Nevertheless, from the negative correlation between zinc line intensity and the frequency of rotation, it is possible they both depend on atomic concentration.

The frequency of rotation and the intensity of the 3076 Zn I spectral line reach a steady state after 6-7 minutes. Once zinc is depleted from the plasma, the frequency of rotation and intensity of the spectral line return to initial conditions. The amount of time necessary to reach a steady state depends on the argon flow rate, the arc current, the magnetic field, and the amount of zinc.

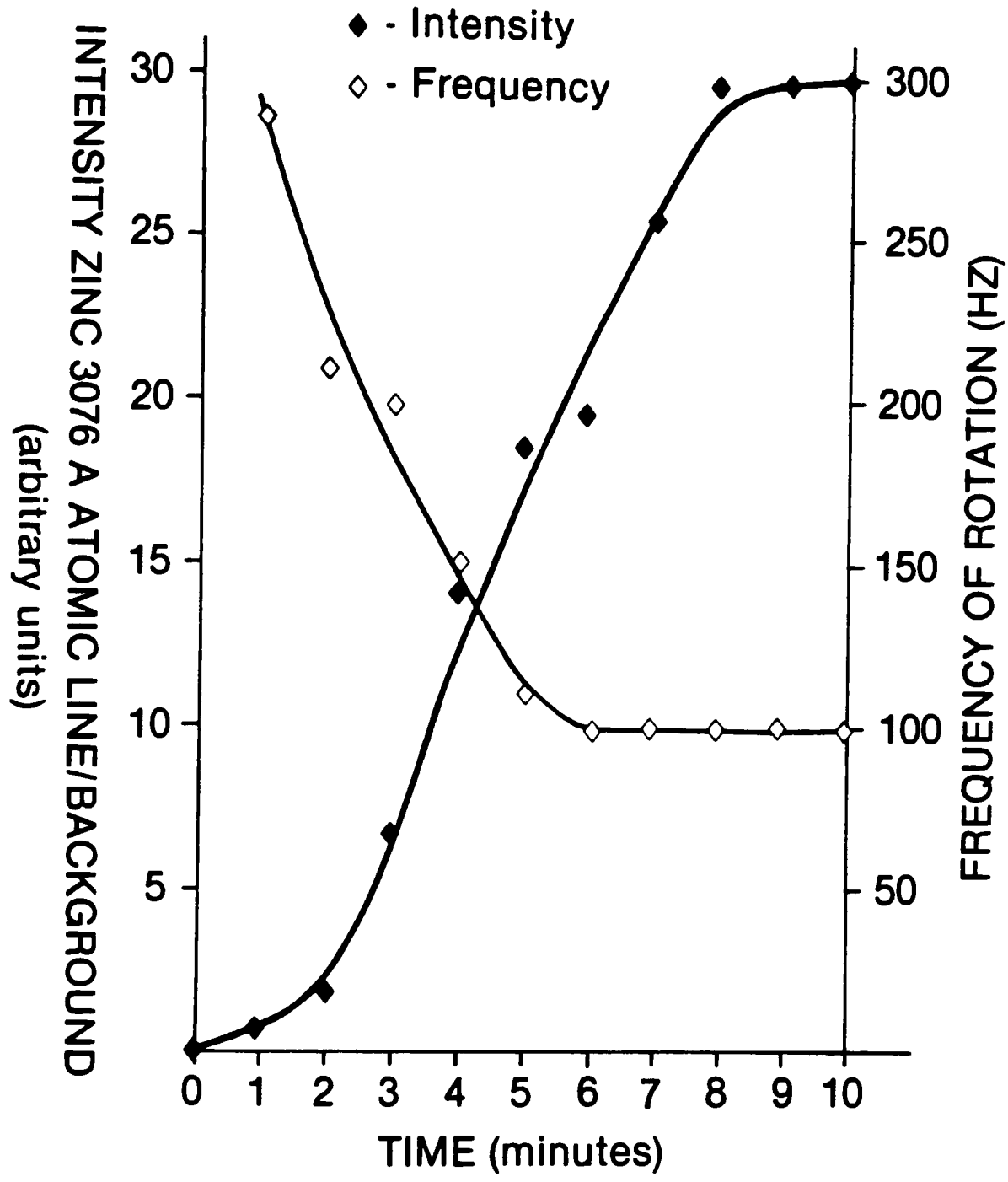

Figure 15
Frequency of Plasma Rotation and the Intensity of the
Zn I 3076 Å Spectral Line as A Function of Time

Spectroscopic experiments were conducted after the achievement of steady state. Steady state conditions were determined from the audible decrease in the frequency of rotation.

2. Thermocouple Determination of Temperatures Inside the Graphite Tube

The temperature of the plasma gases inside the graphite tube was measured with a thermocouple. The signal depended on many factors including the arc current, heat conduction, and convection of the plasma, heat capacity of the anode tube, and heat conduction and heat capacity of the thermocouple[27].

Potential problems associated with thermocouple measurements in general are corrosion, electrical noise, and conductive and radiative cooling of the temperature probe. In the argon/zinc plasma, zinc tends to coat the thermocouple and could be a problem. Otherwise, corrosion was not a problem. Temperature measurements around the anode with the power supplies on and off indicate that electrical interference was not a problem for measurements made outside the anode tube. It is difficult to determine whether this is true inside the anode tube since all the power supplies cannot be turned on without igniting the source. And neither conductive nor radiative cooling of the thermocouple

is a problem due to the large forced convection of the gas and small diameter of the thermocouple.

A gradual increase in temperature is realized after the temperature of the flowing gas is stable due to the gradual increase in temperature of the entire apparatus. All temperature measurements reflect this temperature rise as a background effect. This can cause uncertainties in the day-to-day reproducibility of the measurements.

Although the exact value of the temperature may not be correct, the changes in the measurements reflect changes in the gas temperature. Also, the temperature measurements provide an indication of the effect of arc parameters.

a. Time Dependence of Argon Gas Temperatures

Figures 16 and 17 show changes in temperature with time after igniting a 3 and 4 A argon arc, respectively, as a function of distance from the cathode tip. Steady state temperatures were observed as a constant maximum temperature after sufficient heating of the source at all distances from the cathode.

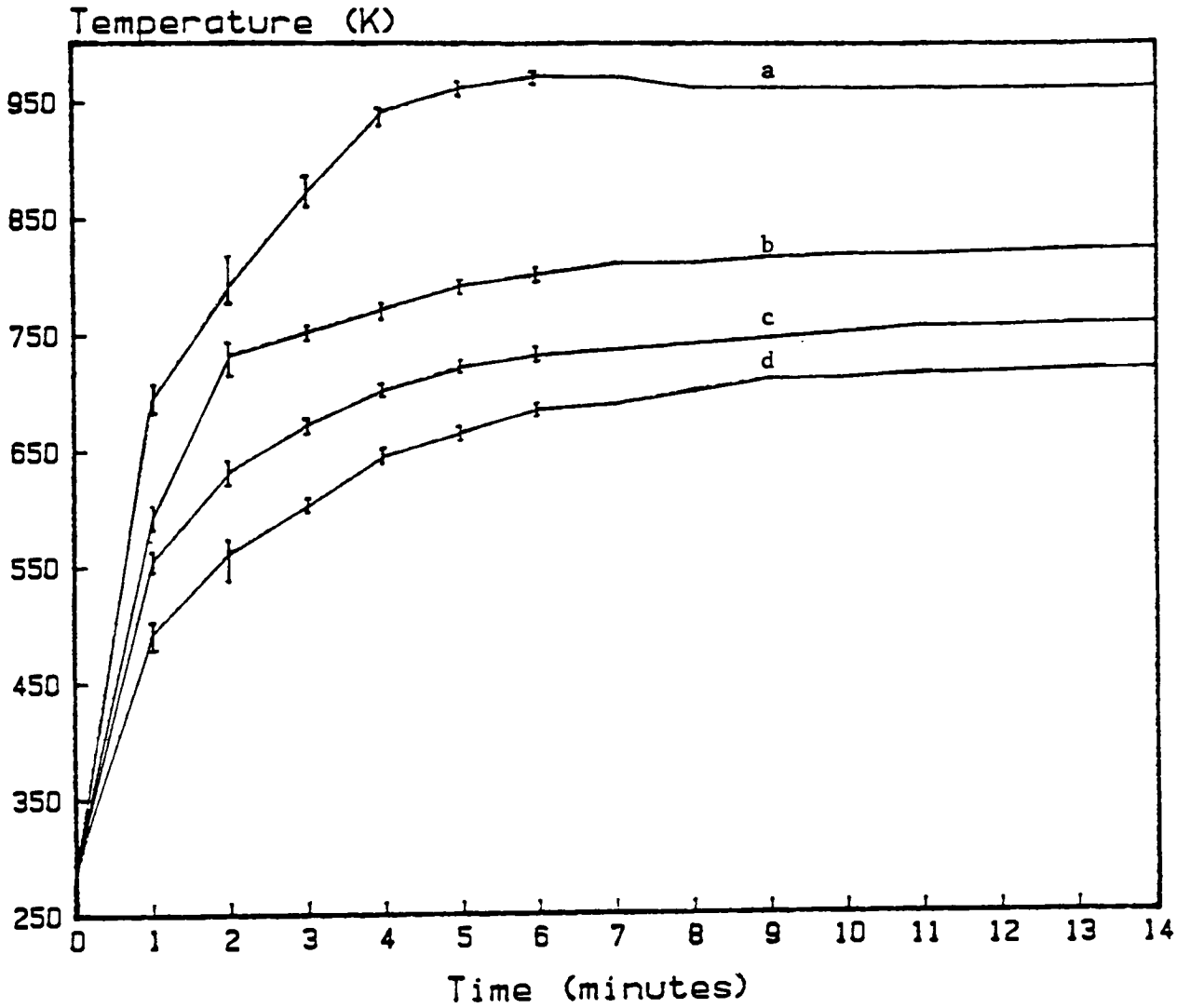

Figure 16
Thermocouple Temperature Measurements of the Argon Gas
as a Function of Time and Axial Distance from the Cathode

The source was operated with a magnetic field of 83 G, an argon flow rate of 1.4 liters/minute, and a source current of 3 A.

Distances from the cathode in mm were:

a - 3.2	c - 9.5
b - 6.4	d - 12.7

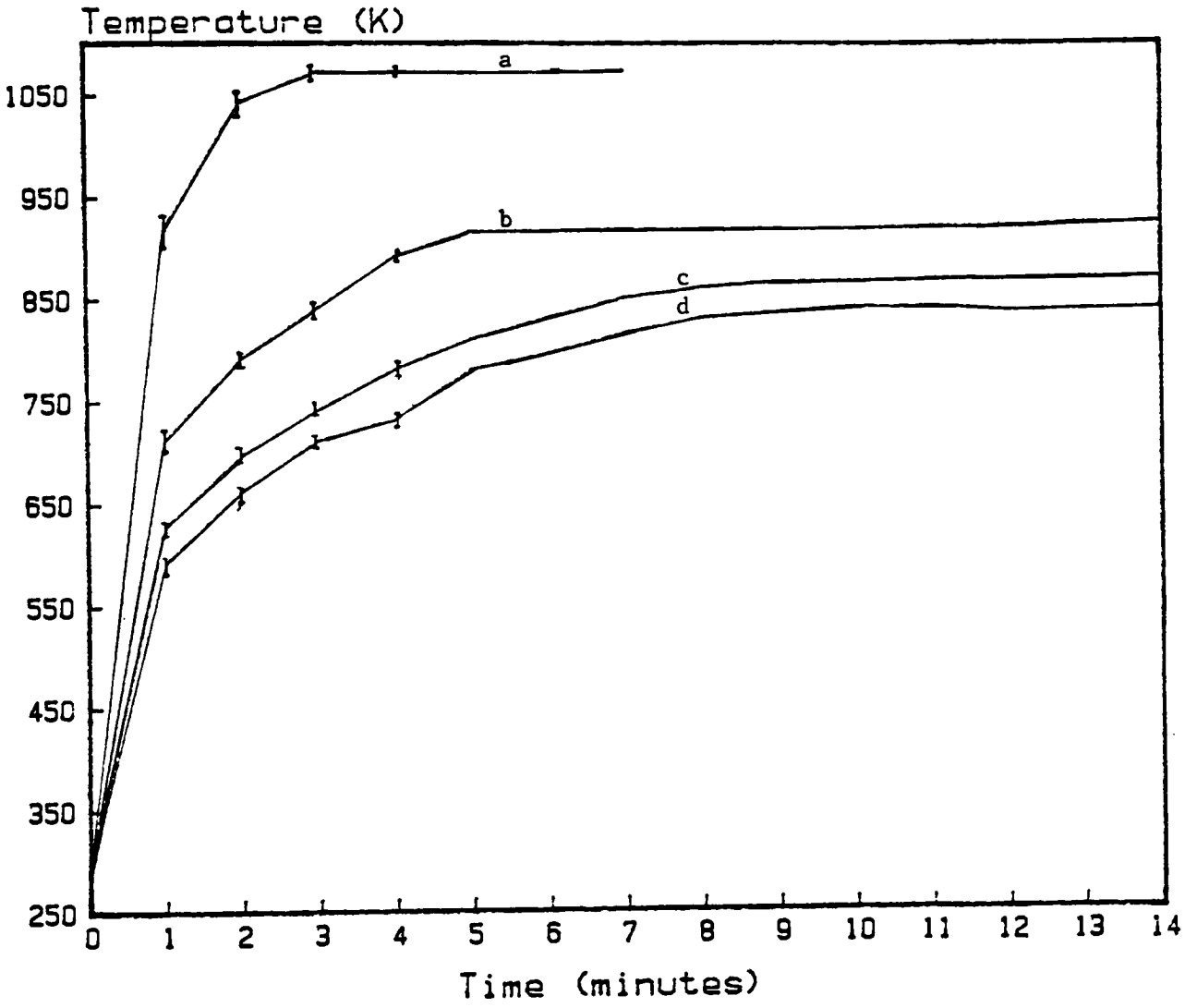

Figure 17
Thermocouple Temperature Measurements of the Argon Gas
as a Function of Time and Axial Distance from the Cathode

The source was operated with a magnetic field of 83 G, an argon flow rate of 1.4 liters/minute, and a source current of 4 A.

Distances from the cathode in mm were:

a - 3.2	c - 9.5
b - 6.4	d - 12.7

b. Argon/Zinc Gas Temperature

Gas temperature are shown in Figure 18 for an argon and an argon/zinc plasma as a function of time. Zinc evaporates into the plasma and achieves a steady state condition with respect to gas temperature as well as the frequency of rotation and atomic spectral-line intensity, discussed previously.

In general, the attainment of steady state is faster for an argon/zinc plasma compared to a similar argon plasma. Zinc has a low melting point, approximately 690 K, and is easily volatilized into the plasma. The temperature measurements also indicate a slight increase in temperature when zinc is added to the plasma. Even though zinc has a high ionization potential, 9.4 eV, it is more easily ionized than argon; thus, the electron density increases.

3. Arc Wandering

A peculiarity of a dc arc that lessens reproducibility is the failure of the arc column to cover the entire surface of the cathode; instead, contact is made only at spots. These contact spots wander erratically and slowly with time, giving the arc an unsteady appearance. Volatilization of a

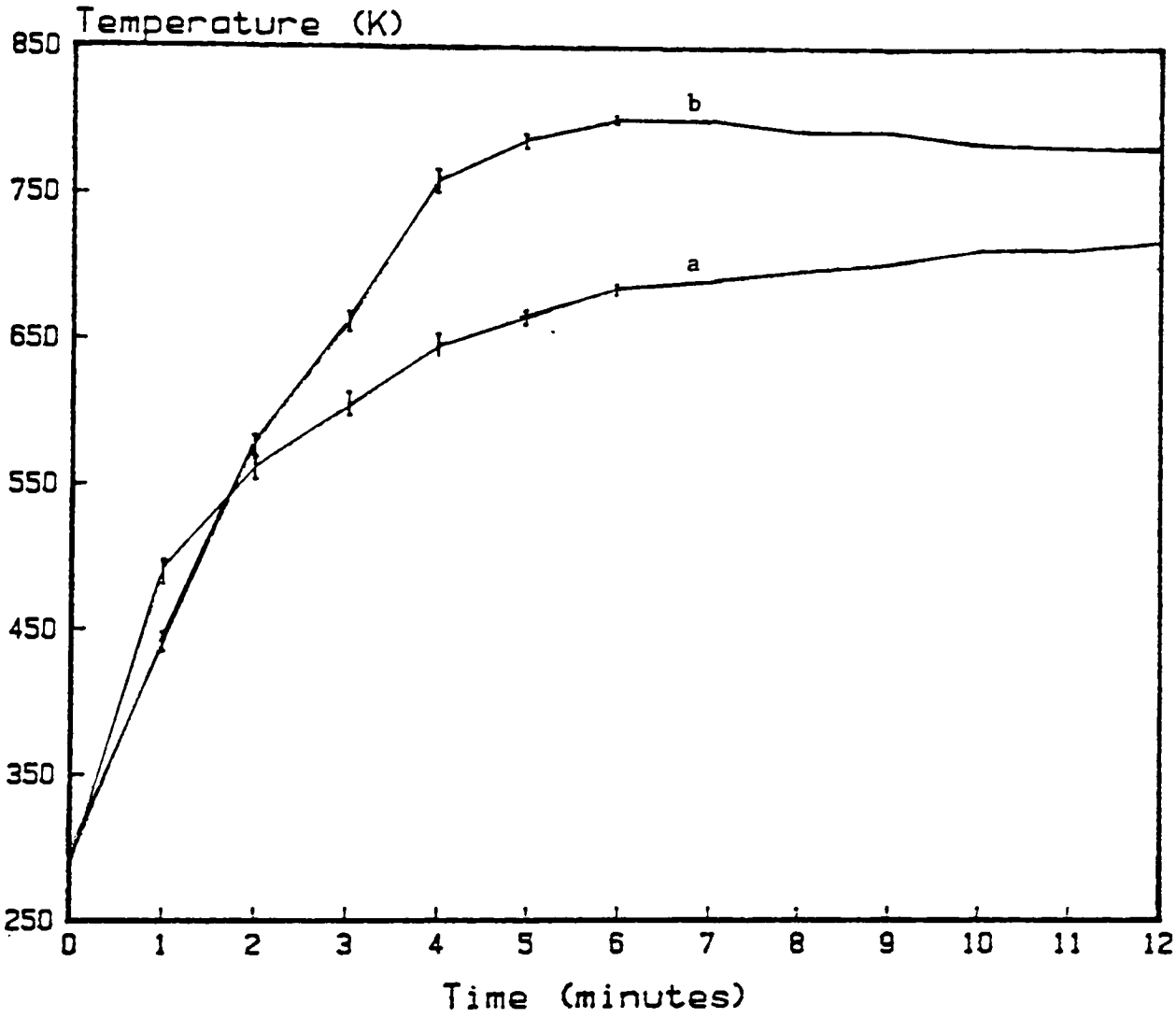

Figure 18
Thermocouple Measurements for (a) Argon and (b) Argon/Zinc Gas at 12.7 mm from the Cathode Tip as a Function of Time

The source operating conditions were a magnetic field of 83 G, an argon flow rate of 1.4 liters/minute, and a source current of 3 A.

sample may contribute to the erratic character of the arc and, conversely, an unsteady burn leads to irregular evaporation. Thus, observed line intensities may fluctuate as a consequence of the movement. The use of magnetic devices are discussed in spectrochemical literature[28] as a technique to stabilize the arc.

Emission intensities were seen to fluctuate with every rotation of the arc. The relative standard deviation of the intensity of the Zn I (3076 Å) spectral-line shown in Figure 8 was 8% for 16 consecutive arc rotations. At times, multiple emission maxima for a single rotation were observed. A high-speed camera showed the arc splitting into several rotating sectors during one rotation[29]. At other times, a maximum emission for an arc rotation was not observed, due to anodic spots. The arc will momentarily stabilize or move erratically to a spot on the anode wall. Even though the arc appears unstable, steady state conditions prevail over relatively longer time periods.

D. Axial Temperature Distribution for an Argon Plasma

The axial, rather than radial, temperatures in an electric arc of coaxial design are meaningful in flow systems used for plasma chemistry. The large mass throughput is desirable for a number of inorganic syntheses since the reactions are quite vigorous[30].

Jacobson and Venugopalan[31] used a similar arc design with nitrogen and air. They found the temperature, T, as a function of the axial distance, x, from the cathode tip could be well fitted using the equation

$$T = m * \log (x) + b$$

where m and b are constants.

The solid lines in Figure 19 show steady state temperatures determined, from Figures 16 and 17, at different distances from the cathode tip. The dotted lines represent the least squares fit of the data using the equation shown above. Experimental results are described by the equation. Thus, the axial temperature profile can be calculated with the determination of 2-4 temperatures in the anode tube for a set of source parameters. Apparently, the equation is unique for the source design since experimental temperature distributions for an argon and a nitrogen arc were duplicated mathematically. That is, the arc composition and source parameters affect the absolute values of the temperature in a predictable distribution.

The axial temperature of the arc decreases more than 400 °K over a distance of 4 mm from near the cathode tip, and an increase of approximately 100 °K was found when the current was increased from 3 to 4 A. The rise is primarily due to higher electrical

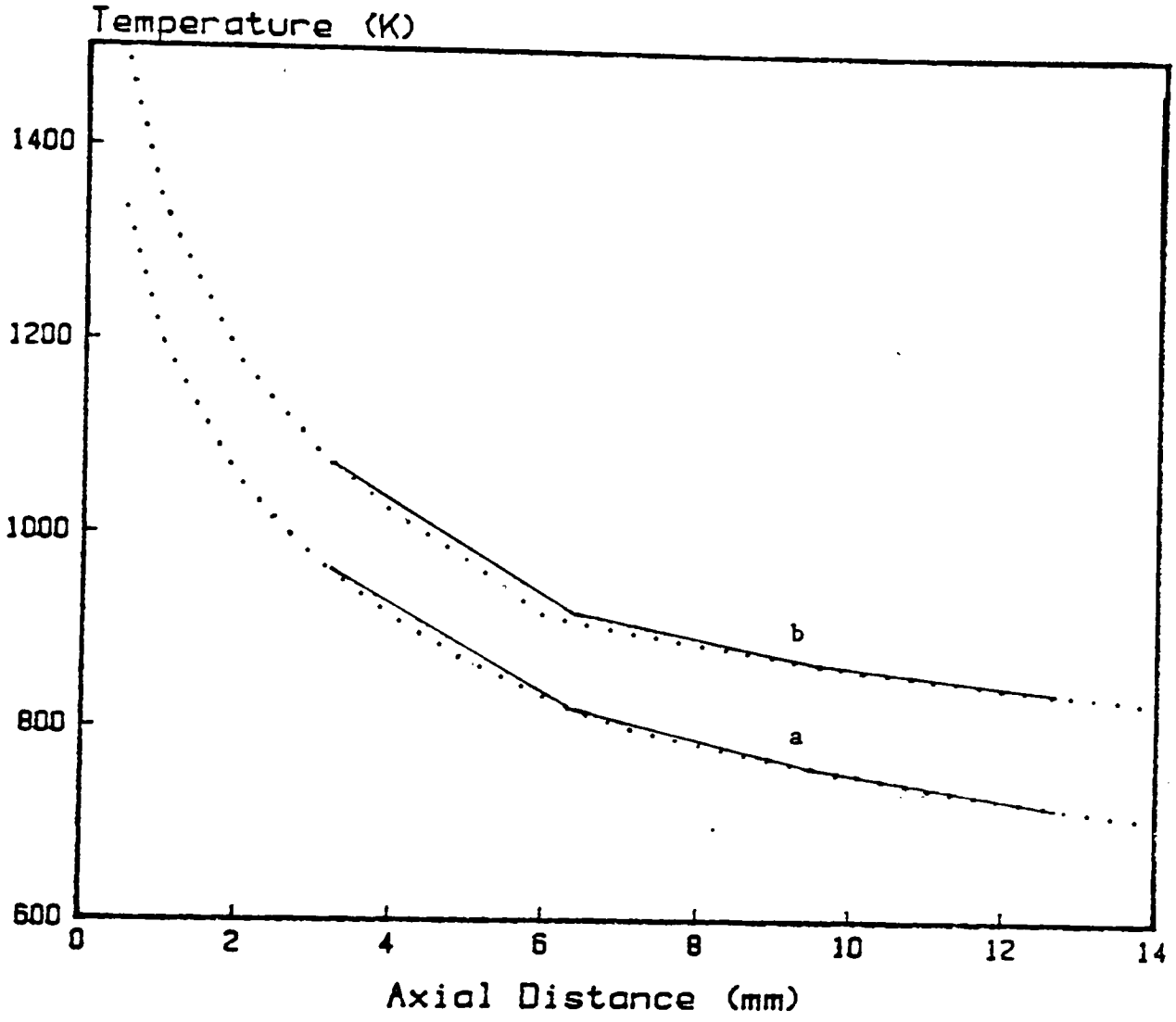

Figure 19
Gas Temperature T as a Function of the Axial Distance X from the Cathode in an Argon Plasma for an Arc Current of (a) 3 A and (b) 4 A

The dotted lines (...) represent a least squares fit of the experimental data (-) using the equation T = m* log (x) + b.

energy supplied to the arc and the energy carried away from it. The heat produced from the arc is carried away to the surroundings via thermal conduction[32].

The total thermal conductivity is given by

$$K = Kn + Kr + Kt$$

where Kn is the thermal conductivity (without reactions), Kr is the thermal conductivity due to transport of reaction energy (including ionization energy), and Kt is the thermal conductivity due to thermal diffusion[33]. The contribution of the third term to the total conductivity is small and can be neglected. The part contributed by the transport of reaction energy is by far the greatest influence on the axial temperature distribution of an arc.

E. Radial Temperature Distribution

The transport of particles, their distribution in the plasma, their dissociation and excitation will considerably depend on the temperature distribution. The radial temperature distribution in the arc influences the spectral-line intensities of the chemical elements, which is the basic interest of spectrochemists. From a spectrochemical point of view, not the line intensities, but their ratio to the background, has to be considered.

The energy available for excitation varies along the length of the arc. Near the electrodes, potential drops over a region of about 1 mm occur related to the space-charge zones at the electrodes. Near the cathode, the plasma energy is highest as a result of a concentration of high-velocity ions, electrons and atoms. For this reason, samples to be examined are placed on the cathode where they are quickly vaporized into the high temperature region. When the gap between the electrodes exceeds a value of about 5 mm, a region of the plasma having a rather uniform potential gradient, current density and temperature develop. A short arc has no uniform column, and the field strength changes continuously from the cathode to the anode.

1. Determination of Temperature from Emission Intensities

   Relative intensities of spectral lines is the most common spectroscopic method for temperature determination. The equation, derived in Appendix III, used for temperature calculations from measurements of the two spectral lines "a" and "b" is

$$T = \frac{5040 \text{ deg} \cdot \text{eV}^{-1} \, (Ea - Eb)}{\log \frac{Aaga}{Abgb} \frac{\lambda b}{\lambda a} + \log \frac{Ib}{Ia}}$$

   where I is the emission intensity measured at a wavelength, λ, described by E, the energy of the excited state, A, the transition probability, and g, the statistical weight of the excited level.

The absolute experimental values of temperature depend largely on the method. Temperatures determined using relative intensities will depend on the relative transition probabilities inserted into the equation. The lack of uniformity in the published data on transition probabilities has been demonstrated by the National Bureau of Standards[34]. Therefore, differences in results for similar arcs may arise from systematic errors in the data on which the measurements are based. Also, comparison of results with the literature are difficult, since operating conditions of a particular source are often insufficiently specified. This applies especially to arcs in inert atmospheres, where results are influenced by the presence of even a few percent of a molecular gas.

a. Equations for Argon Spectral-Lines

Equations (1) and (2) were used to calculate temperatures for atom-atom line pairs Ar 3649.83/3948.98 and Ar 3649.83/4272.17, respectively. The equations are based on the spectral data[35] shown in Table 1.

$$T = \frac{2671.2 \text{ deg}}{-0.1828 + \log \frac{Ib}{Ia}} \qquad (1)$$

where a = 3649.83 Å
b = 3948.98 Å

$$T = \frac{3528.0 \text{ deg}}{0.4036 + \log \frac{Ib}{Ia}} \qquad (2)$$

where a = 3649.83 Å
b = 4217.17 Å

Table 1
Transition Probabilities for Argon I Spectral Lines[35]

Wavelength (Å)	Absorption Transition	Energy of Transition (eV)	Transition Probability (Sec^{-1})	Statistical Weight Upper Level
3649.83	$4s'\left[\frac{1}{2}\right]^{\circ} \text{-->} 6p'\left[\frac{1}{2}\right]$	11.83-->15.22	0.85×10^{6}	1
3948.98	$4s\left[1\frac{1}{2}\right]^{\circ} \text{-->} 5p'\left[\frac{1}{2}\right]$	11.55-->14.69	4.67×10^{5}	3
4272.17	$4s\left[1\frac{1}{2}\right]^{\circ} \text{->} 5p\left[1\frac{1}{2}\right]$	11.62-->14.52	0.84×10^{6}	3

b. Equation for Zinc Atom Spectral-Lines

Equation (3) was used to calculate temperatures for the atom-atom line pair Zn 3075.90/3072.06. The energies of the excited states are 8.11 and 4.03 eV for the atomic zinc lines at 3072.06 and 3075.90 Å, respectively[36]. The relative transition probability is 380[37] in air at atmospheric pressure.

$$T = \frac{20{,}563.1 \text{ deg}}{2.58 + \log \frac{Ib}{Ia}} \qquad (3)$$

where a = 3072.06 Å
b = 3075.06 Å

2. Detector Calibration

a. Photomultiplier Tubes (PMT's)

The maximum response difference between PMT's was 13%. The intensity of the weakest argon line, 3649.8 Å, was detected with the most sensitive PMT.

b. Film Calibration

The response of the emulsion at 3076 and 3072 Å is shown in Figure 20. The optical densities for the exposures shown were constant the length of the exposed slit and from 3070 to 3078 Å. The response is useful over a relatively short dynamic range compared to a PMT, about two decades of intensities, typical for a relatively high contrast emulsion. The speed of the emulsion is slow since the linear range requires very high exposures.

3. Self-Regulation of Temperature in the Arc Column

The electrical conductivity of a gas in an arc is the result of the high temperature. Electrons and ions originate from thermal ionization of the gas mixture in the column. Under the influence of the electrical field, the charge carriers move through the plasma. The electrons migrate toward the anode and the ions migrate toward the cathode. Because of their small mass and high mobility, the electrons carry more than 99% of the current. Therefore, the arc column is a

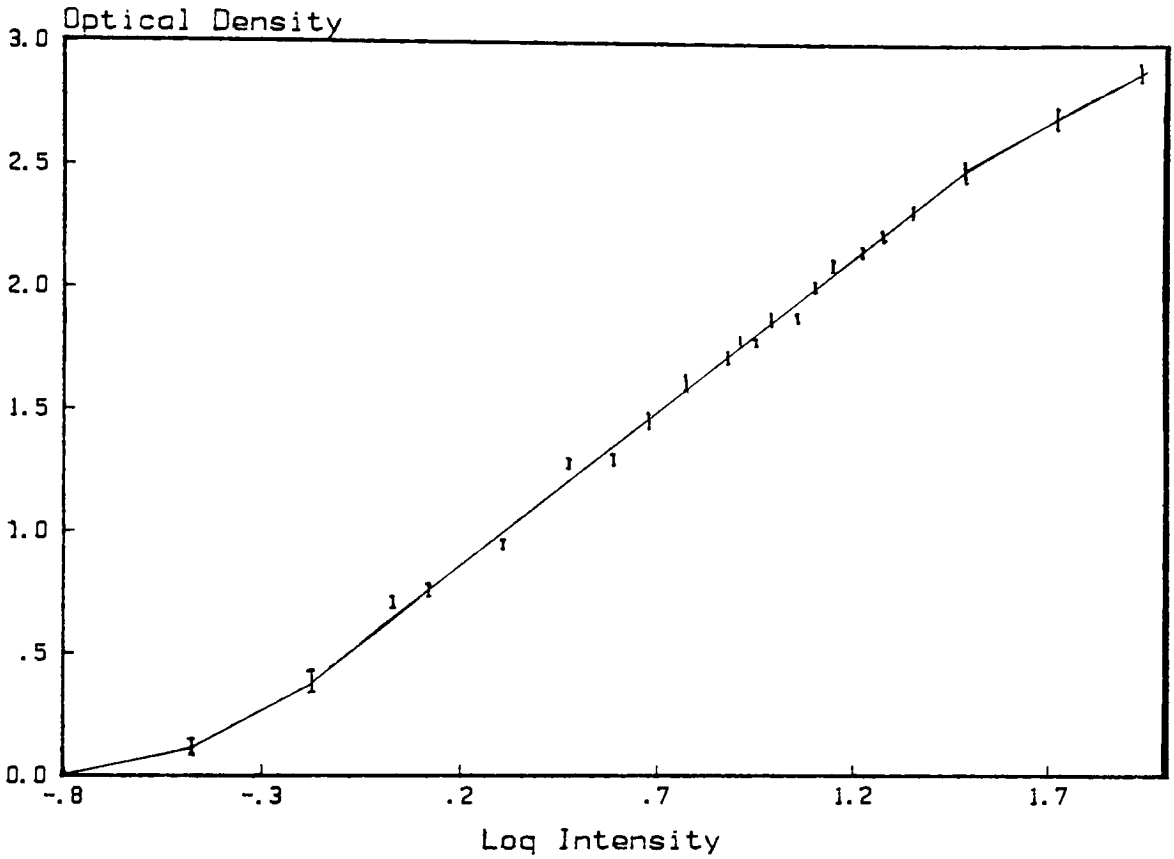

Figure 20

Calibration Curve of Eastman SA No. 1 Photographic Emulsion for the Wavelength Range 3070 to 3078 Å

steady system in which the cathode supplies the same number of electrons as the anode absorbs per unit time. This flow of electrons heats the gas and maintains the elevated temperature required to retain electrical conductivity.

The arc column is a cylinder uniformly filled with a gas mixture of a given composition and pressure for a given radius. The electrical conductivity of the gas is:

$$\sigma = e\ ue\ ne\ \pi\ R^2$$

where e is the electronic charge, ue is the electron mobility, ne is the electron concentration, and R is the radius of the column. The dominant parameter of σ is ne. For a gas of fixed composition and pressure, ne depends only on the temperature; it increases steadily with T.

The heat produced by the electrical current flows away to the surroundings via thermal conduction. The arc takes up the precise temperature at which the power supplied equals the energy loss by thermal conduction. Both functions depend primarily on the gas composition.

Thermal conduction is virtually unaffected by the presence of added metal vapors because the proportion of the vapors in the plasma does not exceed a few percent[38]. However,

the power dissipation is very sensitive to small additions of elements to the arc plasma. The presence of even a small amount of an element having a low ionization potential will furnish electrons more easily than the other gas components. Thus, the value of ne required to retain the electrical conductivity is achieved at a lower temperature than in the absence of the added substance.

An important feature of an arc is the restricted range of values that the electron concentration can assume[39]. Due to the self-consistency of thermal ionization in a normal low-current arc, T is in the range of 4000 to 7000 K, ne ranges from about 10^{14} to several times 10^{15} electrons/ cm^3, and the electron pressure ranges from 10^{-4} to 10^{-3} atm.

4. Radial Temperature Distribution in an Argon Plasma

Nubbemeyer[40] reported temperatures for an LTE argon-arc plasma between 10,000 and 20,000 K and deviations from LTE for electron number densities less than $10^{23}/m^3$ using a wall-stabilized arc between 20 and 240 A. Houwelingen[41] measured radiance of spectral-lines emitted by an argon-arc discharge at 75 and 100 A in a sealed tube to determine temperatures of 11,050 and 11,530 K, respectively.

However, at current strengths less than about 15 A, departures from LTE are observed for arcs in inert atmospheres. Gurevich and Podmoshenskii[42] reported a temperature of 6000 K for a 5 A carbon arc in air at atmospheric pressure, and 7500 K for a similar arc in argon. Measurements by Tveekrem[43] of carbon arcs in helium and argon yielded results ranging from 5300 to 8500 K in helium and 4800 to 9000 K in argon, depending on the thermometric species and the data reduction.

The conditions most favorable for the population of a level to conform with Boltzmann's law are a low excitation energy and a high electron temperature. The larger the arc current, the closer a state of equilibrium is approached, since the electron concentration increases when the current is raised.

The temperature distribution for a 4 A argon arc was determined by averaging results obtained from Equations (1) and (2) and the corrected spectral-line intensities. Figure 21 shows the temperature distribution of the arc column; the regions near the cathode and anode tube were not determined. The intense continuum emitted from the cathode and its reflection from the anode tube saturated the

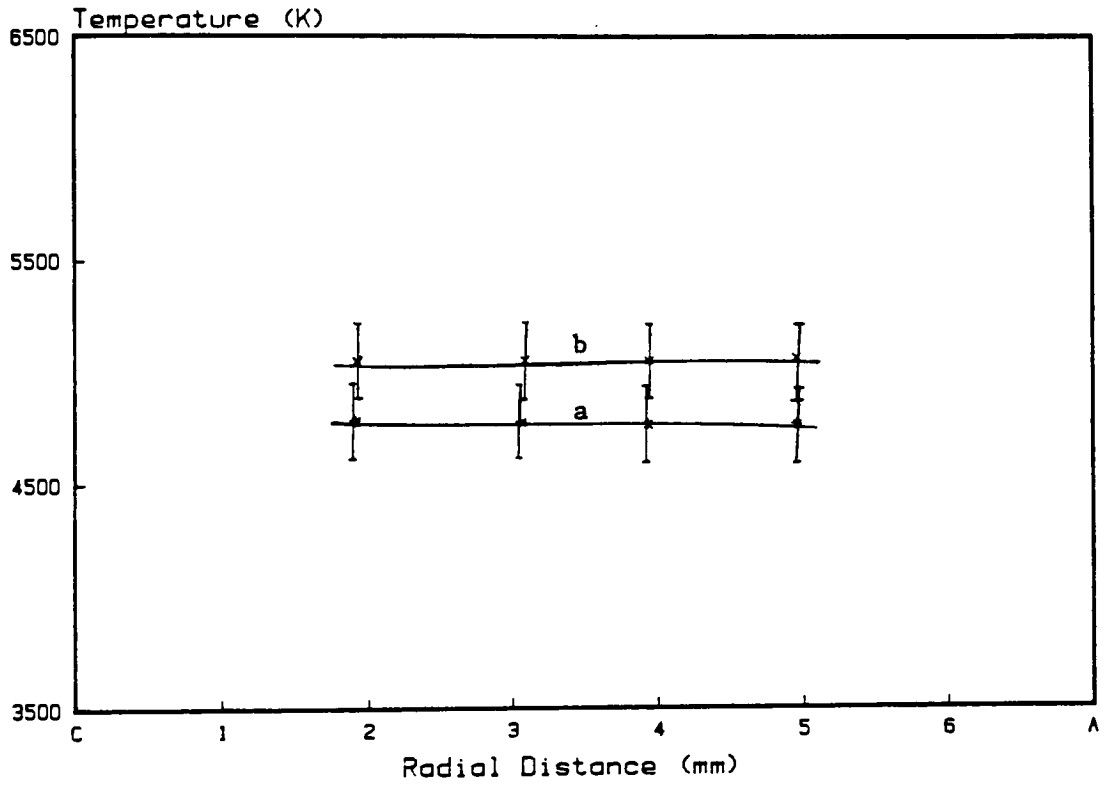

Figure 21
Average Radial Temperature Distribution of an Argon Arc Determined from the Ratio of the Intensities of the Ar Atom Pairs 4272.2/3649.8 and 3949.0/3649.8

Source parameters were: An arc current of 4 A, a magnetic field of 83 G, and (a) 2.6 liters/minute, (b) 2.8 liters/minute.

photomultiplier tubes. Temperature results ranged from 4900 to 5300 K, approximately, for a 4 A argon arc at atmospheric pressure. The radial temperature distribution of argon was not affected by a change in the flow rate from 2.6 to 2.8 liters/minute within experimental error.

The radial emission intensities of the spectral-lines and the background decreased from the cathode to the anode. Atomic emission of argon at 3649.8 Å, the highest energy spectral-line, was not detectable 6 mm from the cathode tip and barely discernable at 5 mm. The ratios of the 3649.8 Å line (corrected for the background)-to-background intensities were virtually constant at 0.3 for the spatial regions investigated. Strong emission intensities were observed for the lower energy argon lines, 3948.98 and 4272.17 Å. Also, the energy of the background radiation was weak, relative to the 3649.8 Å spectral-line at all distances between the cathode and anode.

5. Radial Temperature Distribution for the Argon/Zinc Plasma

a. Determination Using Argon Spectral-Lines

The emission of argon was greatly affected by the introduction of zinc. The lower temperatures obtained when zinc was present did not afford a sufficient amount of argon emission for successive cross sections between

the cathode and anode. The effective or population-averaged temperature was determined with argon lines to be 4700 $\pm$ 250 K, approximately. Effective values are spectroscopic averages over the arc cross section. The temperature depends on the ionization potential of the element. The use of the effective values for characterizing the excitation conditions of other elements is bound by spatial restrictions. The effective temperature is lower compared to temperatures determined in the absence of zinc due to the self-regulating nature of the system.

b. Varying the Concentration of Zinc

The temperatures were found to decrease as the amount of zinc placed in the cathode increased, Figure 22. This relation is characteristic of the arc plasma, an additional increase of zinc would further reduce the temperature only slightly, and the temperature approaches a value characteristic of the ionization potential of the element.

Volatilization is the first step in sample excitation and the rate of evaporation may cause variation in quantitative spectrochemistry. The number of particles

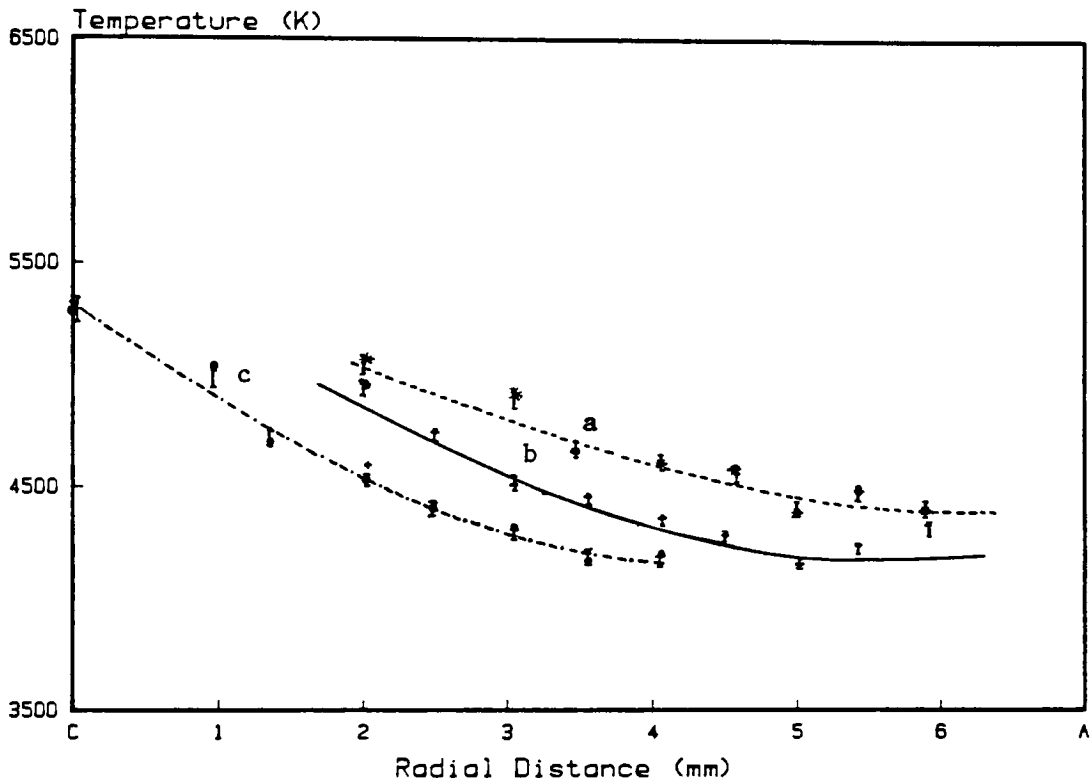

Figure 22
Radial Distribution of Temperature Between the Cathode, C, and Anode, A, for an Argon/Zinc Plasma as a Function of Zinc Concentration

Source parameters were a magnetic field of 183 G, arc current of 5 A, and an argon flow rate of 1.9 liters/minute.

Weight (mg) of Zinc: (a) 10
(b) 15
(c) 20

present in the observation zone is proportional to the rate of evaporation of the element and the intensity is consequently also proportional to the rate of evaporation.

The proportionality between intensity and concentration should apply since the establishment of steady-state, in terms of emission intensity, was shown for zinc. Also, an increase of the integral residence time of the analyte particles in the plasma is achieved in the source, ultimately increasing the probability for excitation. The low melting and boiling points of zinc ensure complete sample volatilization.

Samples with different physical properties may require an alternate technique for sample evaporation.

c. As a Function of Arc Current

At low argon flows, an increase in arc current increases the temperature throughout the source radius as shown in Figure 23. The field produces more electrons when the arc current is increased, heating the gas species in the column. The temperature increase is about 100°K/A.

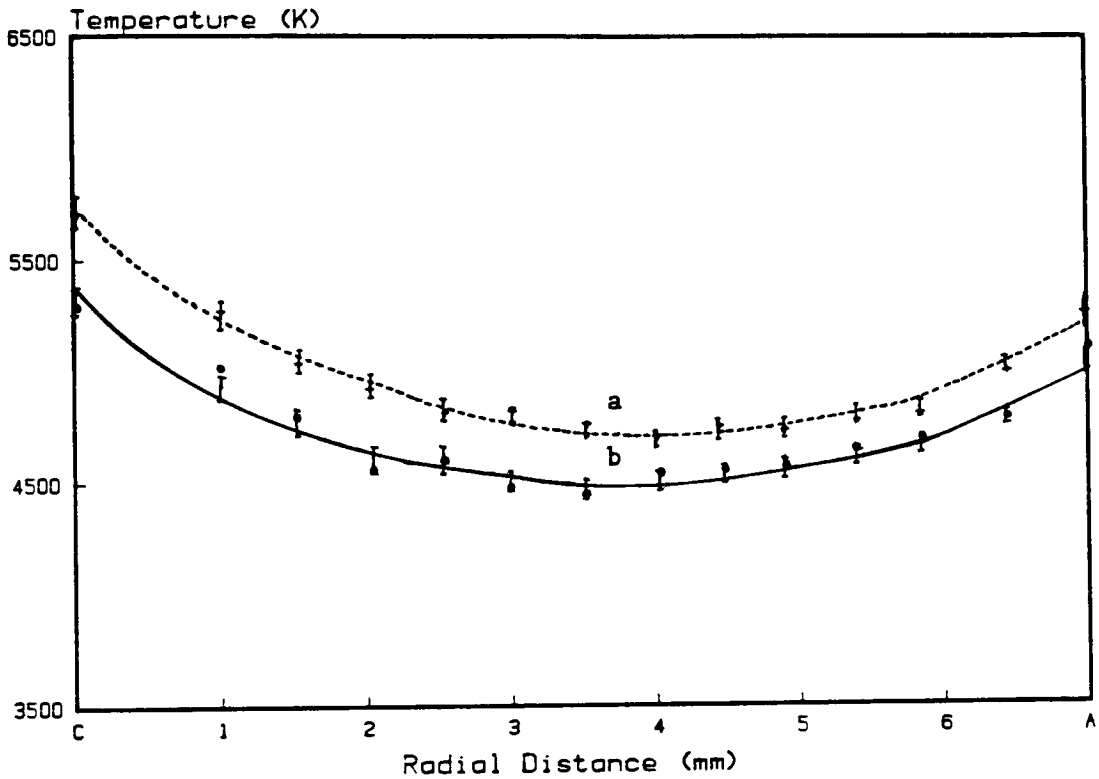

Figure 23
Radial Distribution of Temperature Between
the Cathode, C, and Anode, A, for an Argon/Zinc Plasma
as a Function of Arc Current

Source parameters were: A magnetic field of 183 G and an argon flow rate of 1.4 liters/minute.

For Arc Currents
(a) 5 A (----)
(b) 2 A (——)

The temperature does not increase to the same degree at higher flow rates of argon for the same increase in arc current. Figure 24 shows a rise of approximately 40°K/A.

d. Effect of Argon Flow Rate

Radial transport is due to the migration of ions in the electrical and magnetic fields and convection resulting from the temperature differences between the arc and surroundings. Diffusion processes which tend to expand the vapors axially in the tube are superimposed on the radial motion.

Metal vapors emerging from the cathode are retained by the field and collected near the cathode. As a result, a region of high vapor concentration develops[44]. Particles escape from the cathode layer by diffusion to the cooler fringes and are carried by convection to the periphery of the arc plasma. The material may diffuse inward, thus prolonging the time the particles spend in the arc.

The argon flow rate influences the residence time of particles in the plasma as well as the diffusion rate. As shown in Figure 25, temperatures in the plasma arc column decrease substantially and are less uniform with increasing argon flow rates.

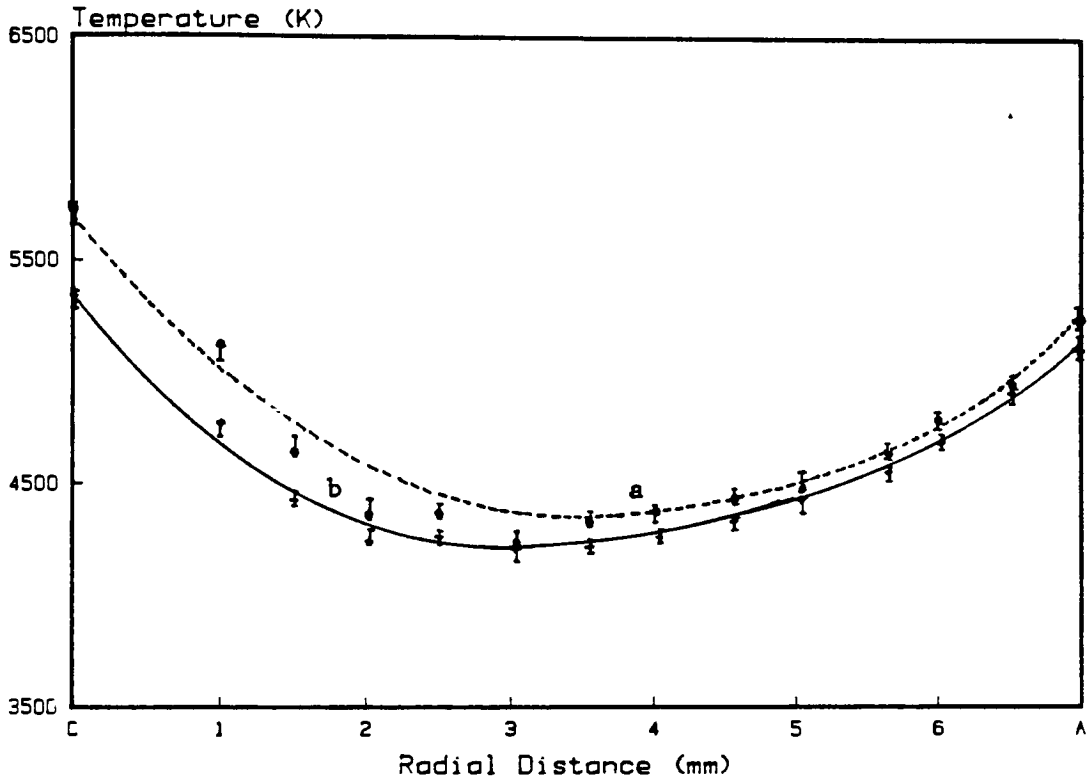

Figure 24
Radial Distribution of Temperature Between
the Cathode, C, and Anode, A, for an Argon/Zinc Plasma
as a Function of Argon Flow Rate

Source parameters were: A magnetic field of 183 G and an argon flow rate of 2.6 liters/minute.

For Arc Currents
(a) 5 A (----)
(b) 2 A (——)

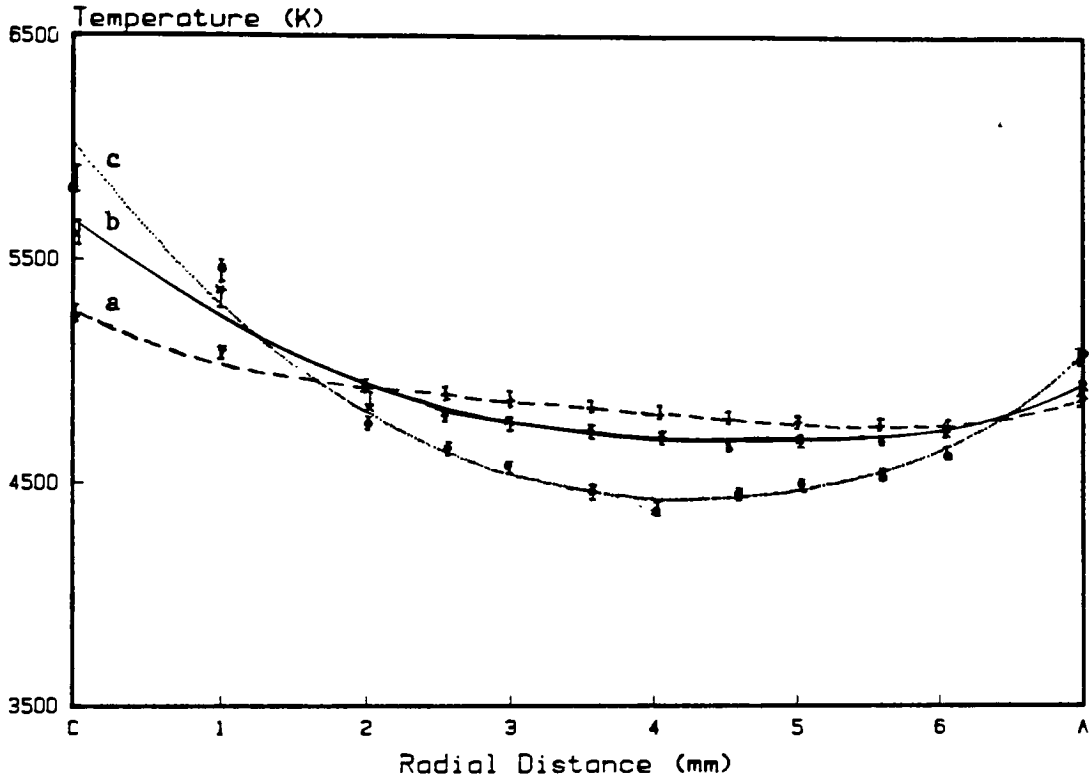

Figure 25
Radial Distribution of Temperature Between
the Cathode, C, and Anode, A, for an Argon/Zinc Plasma
as a Function of Argon Flow Rate

Source parameters were: A magnetic field of 83 G and an arc current of 4 A.

For Argon Flow rates (liters/minute)
(a) 1.4 (----)
(b) 1.9 (——)
(c) 2.8 (·····)

Unfortunately, the temperature distribution is in only two dimensions; zinc emits from a large volume which includes that dimension not obtained. The cooling effect of the gas stream makes the peripheral regions of the arc less conductive and constricts the arc channel, and the gas temperature increases. Thus, a greater electron density results and, consequently, a decrease in electron temperature.

The axial diffusion of zinc causes the absolute temperature to vary less steeply throughout the radius, but discrepancies could result from different rates of diffusion.

e. Magnetic Field Strength

There was no measurable change in temperature, within experimental uncertainty, as the magnetic field strength was changed. The magnetic field causes the plasma arc to rotate, and the frequency of rotation depends on the magnetic induction and arc current. The ions, because of charge neutrality, rotate with the electrons in the magnetic field. The neutral particles diffuse out of the plasma and can reenter the plasma sector several times as it rotates. Thus, rotation of the plasma contributes to the probability of the investigated

particles becoming involved in the discharge column. Hopefully, this process produces a more reproducible source because it minimizes many of the time-dependent changes that occur in the normal dc arc.

Investigations[45] with a high speed camera indicate that the frequency of rotation is also influenced by the phenomena near the anode. The plasma does not rotate smoothly because of its tendency to maintain a former anodic spot. As the anode gets hotter, the rotation frequency increases to a saturation value where a state of steady rotation prevails (Figure 15).

The intensity of zinc emission near the anode surface was slightly enhanced at high applied magnetic fields. This is associated with the process of back evaporation of analyte particles from the tube surface. As a result, an increase of the integral residence time of the analyte particles in the plasma was achieved. The effect of back evaporation in the arc source has been considered as one of the main factors contributing to low values of the detection limit[46].

6. Uncertainty of Results

The random or experimental errors are inherent in any measurement and are just as likely to cause the result to be too high as to be too low. Regardless of how carefully the measurements are made, there will be some variability between successive measurements of a quantity[47].

The relative (or fractional) error in temperature, eT, is shown in Appendix IIIB to be

$$\frac{eT}{T} = \frac{k}{Ea - Eb} \qquad \frac{e\ (Ia/Ib)}{Ia/Ib}$$

where E is the energy of the upper level in eV, I is the intensity of the respective spectral line, e (Ia/Ib) is the absolute error in the intensity ratio measurement and $k = 8.617 \times 10^{-5}$ eV/deg.

The error in temperature is dependent on the difference in energies of the spectral lines and the experimental error of their ratio determination. The relative error in the intensity ratio is nearly constant for the detection method at wavelengths a and b. Thus, the uncertainty in the determination of temperature will be minimized with a large difference in spectral-line energies. A larger uncertainty in temperature is expected using argon spectral lines, compared to zinc, since the energy difference is smaller by an order of magnitude.

The relative percent error in the spectral-line intensities was approximately 15% for argon and 10% for zinc. The absolute error in temperature was approximately 500 K and 50 K for argon and zinc spectral-lines, respectively.

IV. DISCUSSION

A. Spectrochemical Source

A rotating, low current argon arc operating at atmospheric pressure was characterized in terms of emission spectra and plasma and gas temperatures. Plasma temperatures were determined between the cathode and anode from the ratio of the powers radiated per unit volume for two spectral lines. Zinc was added to the plasma to optimize the source parameters for spectrochemical analysis.

Photographic detection of spectra lines was generally utilized for quantitative temperature measurements of the plasma. Eventhough the technique is manually labor intensive, it was found to be precise for determination of emission intensities between the cathode and anode. Random fluctuations in the emission signals caused by small changes in conditions and many variables in volatilizing and exciting atoms were averaged over several seconds to a meaningful and reproducible quantity. In addition, the photographic method was more precise and accurate for distribution measurements than the photoelectric method, due to tedious optical alignments and uncertainties in volume determinations.

large influence of the source and source conditions upon both the pattern and the intensity of lines produced by a species. It is apparent that the source serves two purposes. First, it must provide sufficient energy to volatilize the sample and convert the individual components to gaseous atoms or ions. The second function is to supply sufficient energy to cause electronic excitation of the elementary particles in the gas. In these processes it is essential that the distribution and excitation of the elements in the vapor be reproducibly related to their concentration or distribution in the sample. Ideally the procedure for effective volitilization and excitation should maximize the rate of volatilization, provide a slow rate of transport through the excitation zone and maximize the temperature without unduly increasing the degree of ionization. The source conditions selected will ultimately depend on the nature and physical characteristics of the sample.

Current is carried in an arc by the motion of the electrons and ions formed by thermal ionization. High temperatures develop in the arc gap as a result of resistance to this motion by the atoms. Although thermal ionization does occur in an arc, the energies are such that neutral particles rather than ions are responsible for most of the radiation. Thermal excitation is governed by the Boltzmann equation where the number of atoms excited to a given quantum level increases exponentially with temperature. Thus, the

arc temperature depends upon the composition of the plasma, which in turn depends upon the rate of formation of atomic particles from the sample and electrodes. If the rates at which various species are evaporated into the arc differ, the composition of the plasma, and therefore the temperature, may undergo variation with time. The arc source operating conditions will also effect the volitalization of a sample and is not easily controlled through instrument design. Variations in volatilization were allowed for by a steady state measurement procedure.

An arc current of 4-5 A is required for complete sample evaporation and attainment of steady state conditions within 5-7 minutes. The intensities of th zinc spectral lines were approximately an order of magnitude weaker at arc currents lower than 3 A. In addition, the achievement of steady state conditons took about 8-12 minutes. The lower applied potential effected either the sample vaporization and transport or thermal excitition or a combination of both processes. Samples having higher melting points than zinc, 420^{o}C, may require even higher arc currents for complete volatilization.

At the higher arc currents the radial temperature distribution of the plasma was more uniform with low argon flow rates, 1.4 liter/minute. Steady state conditions also previal longer with low flow rates because gas flow entry is perpendicular to the arc.

The overall cooling effect of high argon rates on the source may be disireable for elements with low ionization potentials, eventhough the useful measurement time would be reduced.

Variations of the applied magnetic field did not absolutely influence the radial temperature distribution. However, rotational frequencies faster than 150 Hz produced a stable and regular rotation with an arc current of 4-5 A. In addition a relatively large volume of high energy was created, since the arc splits to contact many different spots on the anode surface. At lower frequencies the arc had a tendency to maintain an anodic spot and suddenly choose another preferential spot.

An argon/zinc plasma operated at a low arc current, 2A, and a high argon flow rate, 2.6 liters/minute, produced a rotational frequency of 125 Hz and a 19 % variation in temperature between the cathode and anode. The temperature distribution is rather inhomogeneous because of slow vaporizaton of zinc into the plasma and fast velocities of particles through the excitation zone. These conditions provide inadequate reproducibility for quantitative elemental analysis.

The optimum performance of the arc source in terms of efficient and reproducible volatilizaton and excitation of zinc was found with an arc current of 4 A and a slow argon flow rate, 1.4

liters/minute. An argon/zinc plasma rotating at approximately 150 Hz was produced with an applied magnetic field current of 2 A. The time integrated temperature distribution between the cathode and anode for this plasma was uniform (Figure 25), with temperature differences about 4 %. From a spectrochemical point of view, in respect to the residence time of particles in this plasma, such an arc is suitable for spectrochemical analysis.

B. Thermochemical Source

Plasma arc devices have been employed as heat sources for furnaces, to generate thermochemical reactions, for raw material processing (crystal growing, material purification, preparation of ultrafine powders and particle spheroidization), in material fabrication processes (coating deposition, spray forming, welding, cutting and piercing operations), and for material testing, as well as for radiation sources.

The inherent characteristics of an arc which provide an ideal environment for generating chemical reactions are as follows[48]:

1. easy attainment and control of high temperatures (around 1000 K and higher);
2. clean flames composed of a single element or mixture of elements;

3. high-velocity transfer rates;
4. high heat transfer rates;
5. high concentration of energy in a small space.

The high temperature environment of the plasma (3000 - 15,000 K) is a source for free radicals, ions, electrons and unusual molecules. The range of intermediate temperatures, around 1000 K and higher, is also interesting, since chemical reactions is this region are vigorous. The molecular species are in a highly activated state and unusual reactions are quite likely, since the normal restrictions governing room temperature reactions are not present.

The hot gas stream of a plasma arc can be the reactant in a chemical reaction or act merely as the heat source. For most applications a reactive gas stream is obtained with a nitrogen or hydrogen arc and an argon or helium arc is a heat source. Solid reactants are either evaporated into the plasma from the electrode or injected as an aerosol. Liquids and gases are ususally introduced as part of the arc gas mixture. Special techniques are required to trap and quench the end products of a reaction which are unstable outside the controlled environment.

A plasma arc can be employed to thermochemically synthesize hydrogen cyanide by a number of methods[49]:

1. Directly from the elements.
2. From carbon and ammonia.
3. From methane and nitrogen.
4. From ammonia and methane.
5. From ammonia and carbon monoxide.

The elemental reaction, $2C + H_2 + N_2 \rightarrow 2HCN$ ($\triangle Hf = -60$ kcal/mole), of a consumable graphite cathode and an arc gas mixture of hydrogen and nitrogen is an effective process.

The plasma arc has also been employed for vapor-gas phase reactions in the preparation of metal nitrides, carbides, oxides, fluorocarbons and phosphonitrilic. For instance AlN is prepared in a nitrogen arc by injecting powered Al or using a consumable Al electrode[50]. Reactions have also been reported[51] for solid and gas decompositions. The major application of solid decomposition reactions are for ore reduction processes. Examples of gas dissociation in an arc are

1. $2NH_3 \rightarrow N_2 + 3H_2$
2. $CH_4 \rightarrow C + 2H_2$
3. $2Al_2O_3 \rightarrow 4Al + 3O_2$

Chemical reactions proceed quite rapidly at high temperatures,

around 1000 K and higher, so that to the nearest approximation an equilibrium state will be attained. The influence of the arc parameters on the chemical conditions of a system can easily be studied over a wide range by using equilibrium calculations. These conditions are dependent on several variables, such as temperature and amounts of initial substances. The composition of a thermally characterized system containing gases, pure condensed phases and liquid and solid mixtures can be adequately described with equilibrium calculations. The axial temperature distribution was shown to be mathematically described for a set of arc parameters from several temperatures at known distances, x, from the cathode tip by $T = m * \log(x) + b$. A thermocouple was used to directly measure gas temperatures at various distances from the cathode. Thus it is possible to obtain, in a theoretical way, a picture of the prevailing chemical conditions in a high temperature system.

C. Suggestions for Future Work

1. Spectroscopically measure the electron concentration from the intensity ratio of an ion-atom line pair of zinc using the Saha relationship. Simultaneously, determine the temperature and compare with results generated from the intensity ratio of the atom-atom line pair of zinc.

2. Analyze the volume emission intensities obtained via photoelectric detection from data acquisition programs with Fourier analysis. The mathematical analysis can resolve a complex wave train into a set of simple sine waves, thus enhancing the S/N ratio.

3. Add an element with a low ionization potential, a spectroscopic buffer, to the plasma and determine the influence on the temperature and electron density of the plasma, and the distribution of these parameters and the residence time of particles in the plasma.

V. ACKNOWLEDGMENTS

I would like to thank all of the people at Abbott Laboratories and Rochester Institute of Technology who encouraged the finalizing of this work. George Fazekas was instrumental in the establishment of the source and helpful in the preliminary experiments. A special appreciation is also sent to Ann Ark, a typing perfectionist, and David Eaton, my mentor.

VI. BIBLIOGRAPHY

1. E. L. Grove, ed., Analytical Emission Spectroscopy, Vol. 1, Marcel Dekker, N.Y., 1972, pp 2-3.

2. F. F. Chen, Introduction to Plasma Physics, Plenum Press, New York, 1974, p 3.

3. V. Vukanovic, "The Establishment of a Plasma Chemistry Laboratory to Enhance Developments in Laser Fusion Technology", Unpublished Work.

4. S. V. Dresiv, ed., "Physics and Technology of Low Temperature Plasmas", Moscow, Atomizdat 1972, English Edition, The Iowa State University Press/Ames. 1977.

5. A. E. Guile, Proc. IEE Reviews, 118, 1131 (1971).

6. M. Todorvic, V. Vukanovic, V. Giorgijcvic, Spectrochim. Acta, 24B, 571 (1964).

7. M. Todorvic, V. Vukanovic, V. Georgijcvic, Spectrochim. Acta, 24B, 571 (1964).

8. G. Eriksson, Acta Chem. Scand., 25 (1971).

9. M. W. Chase, J. L. Curnutt, A. T. Hu, H. Prophet, A. N. Syrezud, L. C. Walker, "JANAF Thermochemical Table,", 1974 Supplement, J. Phys. Chem. Ref. Data, 3, 331 (1974).

   M. W. Chase, J. L. Curnutt, H. Prophet, R. A. McDonald, A. N. Syvezud, "JANAF Thermochemical Tables", 1975 Supplement, J. Phys. Chem. Ref. Data, 4, 1 (1975).

   D. R. Stull, H. Prophet, et. al., "JANAF Thermochemical Tables", 2nd ed. NSRDS-NBS-37, 1971.

10. M W. Chase, et. al., "JANAF Thermochemical Tables", The Dow Chemical Company, 1978.

11. "Termodinamicheskie Svotstva Individual Veshchestro", Vol. 1, Part 2, 1978.

12. V. Vukanovic, et. al., "A New Direction in Plasma Chemistry for the Coating of Laser Fusion Targets", Unpublished Work, 1981.

13. W. F. Meggers, C. H. Corliss and B. F. Schribner, "Tables of Spectral-Line Intensities", 2nd ed., Part 1, NBS, 1975.

14. G. P. Harrison, "Wavelength Tables", John Wiley and Sons, New York, 1939.

15. "Temperature Measurement Handbook", OMEGA Engineering Inc., 1981.

16. "Kodak Plates and Films for Scientific Photography", 1st ed., Kodak Publication No. P-315, 1973.

17. H. A. Strobel, Chemical Instrumentation: A Systematic Approach, 2nd ed., Addison-Wesley Publishing Co., Mass., 1973, p 386.

18. "Kodak Plates and Films for Scientific Photography", 1st ed., Kodak Publication No. P-315, 1973.

19. N. H. Nachtrieb, Principles and Practice of Spectrochemical Analysis, McGraw-Hill Book Co., Inc., New York, 1950, p 109.

20. P. W. J. M. Boumans, Theory of Spectrochemical Excitation, Adam Hilger, London, 1966; Plenum, New York, 1966.

21. N. H. Nachtrieb, Principles and Properties of Spectrochemical Analysis, McGraw-Hill Book Co., Inc., New York, 1950, pp 135-139.

22. G. Fazekas, R.I.T. Research Notebook and Programs "AVG3" and "SCAN".

23. H. H. Willard, L. L. Merritt, Jr., J. A. Dean, F. A. Settle, Jr., Instrumental Methods of Analysis, 6th ed., D. VanNostrand Company, New York, 1981, p 135.

24. W. L. Wiese, M. W. Smith, B. M. Glennon, "Atomic Transition Probabilities", Vol. 1, NSRDS-NBS 4, 1966.

25. R. C. Weast (ed.), "Handbook of Chemistry and Physics", 56th ed., Chemical Rubber Company, Cleveland, Ohio, 1975, p D-174.

26. H. H. Willard. L. L. Merritt, Jr., J. A. Dean, F. A. Settle, Jr., Instrumental Methods of Analysis, 6th ed., D. VanNostrand Company, New York, 1981, p 158.

27. V. Vukanovic, "A New Direction in Plasma Chemistry for the Coating of Laser Fusion Targets", A Summary Report of Activities by the Plasma Chemistry Group at Rochester Institute of Technology, September 30, 1981.

28. V. M. Vukanovic and V. M. Georgyevic, Z. Anal. Chem., 225, 137 (1967).

29. V. Vukanovic, D. Vukanovic and M. Simic, Spectrochimica Acta, 26B, 481 (1978).

30. M. Venugopalan, International Workshop on Plasma Chemistry in Technology, Ashklon, Israel, April 1981.

31. A. J. Jacobson, M. Venugopalan and V. Vukanovic, International Symposium of Plasma Chemistry, Eindhoven, July 1985.

32. E. L. Grove, ed., Analytical Emission Spectroscopy, Vol. 1, Marcel Dekker, N.Y., 1972, p 20.

33. V. Vukanovic, N. Ikonomov and B. Pavlovic, Spectrochimica Acta, 26B, 95 (1971).

34. C. H. Corliss and W. R. Bozmann, "Experimental Transition Probabilities for Spectral Lines of Seventy Elements", Nat. Bur. Std. Monograph 53, Washington, D.C., 1962.

35. W. L. Wiese, M. W. Smith, B. M. Glennon, "Atomic Transition Probabilities", Vol. 1, NSRDS-NBS 4, 1966.

36. C. W. Hetzler, R. W. Borman, and K. Berus, Phys. Rev., 48, 656 (1935).

37. J. W. Schuttevaer and J. A. Smit, Physica, 10, 502 (1943).

38. P. W. J. M. Boumans, Theory of Spectrochemical Excitation, Adam Hilger, London, 1966; Plenum, New York, 1966.

39. L. S. Ornstein, H. Brinkman and A. Beunes, Z. Physik, 77, 72 (1932).

40. H. Nubbemeyer, J. Quant. Spectrosc. Radiat. Transfer, 16 (1976).

41. D. VanHouwelingen and A. A. Kruthof, J. Quant, Spectrosc. Radiat. Transfer, 11 (1971).

42. D. B. Gurevich and I. V. Podmoshenskii, Opt. Spectry. (USSR) (English Transl.), 15, 319 (1963).

43. M. Margoshes, "Proc. 12th Colloq. Spectrosc. Intern., Exeter 1965", Adam Hilger, London, 1965, p 26.

44. P. W. J. M. Boumans, Proc. 6th Colloq. Spectros. Intern., Amsterdam, 1956, Spectrochim. Acta., 11, 146 (1957).

45. V. Vukanovic, D. Vukanovic and M. Simic, Spectrochimica Acta, 33B, 481 (1978).

46. H. Moller, M. Mazurkiewicz and H. Nickel, KFA-Report Jul-1449, August (1977). H. Moller, Thesis, Technical University, AAchen (1977).

47. D. A. Aikens, et. al., Integrated Experimental Chemistry, Vol. 1, Allyn and Bacon, Inc., Boston, 1978, p 43.

48. P. M. Tyler, J. Metals, 13, 51-54 (1961).

49. E. J. Hellund, The Plasma State, Reinhold, New York, 1961.

50. A. R. Moss and W. J. Young, Powder Met., 7, No. 14, 261-289 (1964).

51. L. N. Hjelm, D. James, and E. Beardsley, AFML-TR-64 398, Air Force Systems Command (1975).

APPENDIX IA - CALCULATIONS OF EQUILIBRIUM PLASMA

The method used by SOLGAS program to determine the composition of an equilibrium plasma is a general one based on the minimization of free energy of the system. The method also eliminates the necessity of writing chemical equations and simplifies the addition and removal of species from the calculation.

The equilibrium composition is that set of non-negative mole numbers which gives the lowest possible value for the total free energy of the system and which satisfies the mass balance constraints. In order to calculate this set of mole numbers, an iterative procedure was used. First, one estimates the number of moles of the substances considered to be present in the system (y°). Improved values of the mole numbers are calculated (Xi) and these are used for a new set (y). This procedure is repeated until the equilibrium composition is obtained. Thus, every iteration starts with a new set of values.

The free energy, G, of the system can be expressed as

$$G = \sum_i X_i g_i$$

where X_i is the mole number of a substance, and g_i is the chemical potential defined as

$$g_i = g_i^\circ + RT \log a_i$$

where the R is the gas constant, T is the temperature, and a is the activity. For gaseous species which are treated as ideal, the activities, a_i, are equal to the partial pressures, p_i

$$a_i = p_i = (X_i/X)P$$

X and P are the total number of moles in the gas phase and the total pressure, respectively. For the condensed substances, which are thought to be pure, the activities are equal to unity. Using the definitions above, a dimensionless quantity (G/RT) can be obtained:

$$G/RT = \sum_{i=1}^{m} Xi^g \left[(g°/RT)_i^g + \ln P + \ln (Xi^g/X)\right] + \sum_{i=1}^{s} Xi^c \, (g°/RT)_i^c \qquad (1)$$

The indices g and c represent the gas phase and condensed phase, respectively. The number of substances in the gas phase is denoted by m, and s is the number of condensed phases assumed to be present at equilibrium.

The value of (g°/RT) is calculated for a certain substance using the expression

$$(g°/RT) = (1/R) \left[(G° - H°_{298})/T\right] + \triangle f \, H°_{298}/RT \qquad (2)$$

where $(G° - H°_{298})/T$ is the free energy function in cal K^{-1} mol^{-1}, and $\triangle f \, H°_{298}$ is the heat of formation at 298.15 K in

cal mol^{-1}. Alternatively, a value of $(g°/RT)$ can be calculated according to the relation

$$(g°/RT) = -\ln 10 \log Kf$$

where Kf is the equilibrium distribution between phases.

The mass balance relations can be written

$$\sum_{i=1}^{m} a_{ij}^{g} X_{i}^{g} + \sum_{i=1}^{s} a_{ij}^{c} X_{i}^{c} = b_{j} \quad (j = 1,2,\ldots l) \tag{3}$$

where a_{ij} represents the number of atoms of the j^{th} element in a molecule of the i^{th} substance, b_j is the total number of moles of the j^{th} element, and l is the total number of elements.

The method involves a search for a minimum value of the free energy of a system, Equation 1, subject to the mass balance relations as necessary conditions, Equation 3. Lagrange's method of undetermined multipliers is suitable, and the following equations are obtained:

$$(g°/RT)_{i}^{g} + \ln P + \ln(X_{i}^{g}/X) - \sum_{j=i}^{l} \pi_{j} a_{ij}^{g} = 0 \quad (i = 1,2,\ldots,m) \tag{4}$$

$$(g°/RT)_{i}^{c} - \sum_{j=i}^{l} \pi_{j} a_{ij}^{c} = 0 \quad (i = 1,2,\ldots,s) \tag{5}$$

The factors π_j are Lagrangian multipliers.

The equations (3) and (4) are expanded in a Taylor series about an arbitrary point

$$(y_1^g, y_2^g, \ldots y_m^g; y_1^c, y_2^c, \ldots, y_s^c),$$

neglecting terms involving derivatives of second and higher orders leads to the following:

$$\sum_{j=1}^{l} \pi_j \sum_{i=1}^{m} y_1^g a_{ij}^a = \sum_{i=1}^{m} fi \qquad (6)$$

$$\sum_{k=1} \pi_k \; r_{jk} + [(X/Y)-1] \sum_{i=1}^{m} a_{ij}^g y_i^g + \sum_{i=1}^{s} a_{ij}^c X_i^c = \sum_{i=1}^{m} a_{ij}^g f_i - C_j$$

$$(j = 1,2,\ldots l) \qquad (7)$$

where $r_{jk} = r_{kj} = \sum_{i=1}^{m} (a_{ij}^g a_{ik}^g) y_i^g \quad (j,k = 1,2,\ldots,l),$

$$Y = \sum_{i=1}^{m} y_i^g$$

and C_j is a correction term in cases where the initial guess of the mole numbers does not satisfy the mass balance relation, equation (3).

Equations (7), (5) and (6) constitute a system of (l+s+1) linear equations, consisting of the (l+s+1) unknown quantities π_j(j = 1,2,...l). X_i^c (i=1,1,....s), and [(X/Y)-1]. The system of equations is solved using Guassian elimination.

APPENDIX IB - DATA FILES FOR CALCULATIONS OF EQUILIBRIUM CONCENTRATIONS FOR USE WITH PRESOL

The data files are easily constructed in the edit mode and subsequently copied into JANAF:DAT(NLN), the JANAF:NDX (index) will be updated along with the data file. A data file is constructed in the following manner:

The first line of each new entry and column numbers is:

	Item	Column Number
1.	Index Number	1-4
2	Compound/Element Abbreviation	5 and 6
3.	Charge (a negative 1 would be 1-)	8 and 9
4.	Number of types of elements in compound	12, 16, 20, 24, 28
5.	Name of element/compound	Begins in 30
6.	State (gas, liquid, solid)	(64)
7.	Molecular weight (with decimal point)	Ends in 74

The thermodynamic data is entered as right justified integers on the second line in the following manner:

	Item	Units	Column Number
1.	Index Number		4
2.	Temperature	degrees K	8
3.	Cp°	$cal \cdot mole^{-1} \cdot deg^{-1}$	14

Item	Units	Column Number
4. DH (H°_{+} - H°_{298})	cal•mole^{-1}	24
5. S^{o}	cal•mole^{-1}•deg^{-1}	34
6. $-(G-H^{\circ}_{298})T$	cal•mole^{-1}•deg^{1}	44
7. H°_{f}	cal•mole^{-1}	54
8. G°	cal•mole^{-1}	64
9. log K	--	74
10. Month-Year	--	80

APPENDIX IC - PROGRAM USED TO RUN SOLGAS

```
!       PRESOL:CMD
```

This command will run the following program. A few questions need to be answered and the estimated equilibrium and initial concentrations need to be assigned before calculations are started.

```
!ECHO

!RESET

!SET F:52/RUNNER:DAT; IN; SAVE
```

File 52 contains the gaseous species to be considered for which data is needed.

```
!SET F:62/COND:DAT; IN; SAVE
```

File 62 contains the condensed species to be considered for which data is needed.

Instructions on the use of the program will be printed. The data tables to be used are designated. The temperature at which the calculations are to be performed is entered. The user must select whether the initial amount of each substance will be grams or moles. As each substance is listed from RUNNER and COND, the computer awaits input of the estimated equilibrium composition and the initial amount. Once the initial and equilibrium amounts are entered, SOLGAS will perform a calculation. Options are given to save the answers and stop SOLGAS.

!SET F:108 ME	Sets the output file to be interactive.
!SET F:10/SOLGAS:DAT:IN; SAVE	SOLGAS data file is saved.
!SET F:12/ANSWERS; OUT; SAVE	Sets up an output file for the final results.
!SOLGAS:LMN	The load module from SOLGAS is printed out. This includes tables of the matrix, formula weights, thermodynamic data used, initial estimates of the equilibrium, and the result table.

```
!SET F:1/MINERAL:DAT; IN; SAVE
```
Reads thermodynamic data in and saves from

```
!SET F:2/JANAF:DAT; IN; SAVE
```
the Mineral and JANAF tables.

```
!SET F:3/MINERAL:NDX; IN; SAVE
```
Reads the indexes in for the corresponding Mineral and

```
!SET F:4/JANAF:NDX; IN; SAVE
```
JANAF tables.

```
!SET F:11/SOLGAS:DAT; OUT; SAVE
```
Results from SOLGAS will be saved.

```
!.Enter NS, BC for options.
```

```
!.FORT PRESOL:F4 OVER PRESOL:REL
```
Presol is converted into a relative program.

```
!.LYNX PRESOL:REL, SUBLIB; REL OVER PRESOL:LMN(JO)
```
The relative program PRESOL is linked to the library and renamed PRESOL:LMN(JO).

```
!PRESOL:LMN
```
The linked program is run. If the program has to be compiled, the periods (.) are left out.

!C ANSWERS TO ME	Prints out the final results as shown in Figure 1. If the estimated equilibrium composition was not close enough to afford a result, a note would be printed at this time.

Figure 1. Sample printout of answers from SOLGAS.

```
INITIAL ESTIMATE OF EQUILIBRIUM COMPOSITION

     COMPOUND                MOLES
     AR 1                .96000E 00
     C  1                .10000E-01
     -  1                .10000E-43
     ZN 1                .20000E-01
     ZN 1                .00000E 00
     C  1                .10000E-19
     ZN 1                .00000E 00
     ZN 1                .00000E 00
T = 3800.00 K
P = 1.000E 00 ATM

                         X*/MOLE          YO/MOLE          Y/MOLE           P/ATM
AR 1                   .96000E 00       .96000E 00       .96003E 00       .96003E 00
C  1                   .20000E-01       .10000E-01       .20000E-01       .20000E-01
-  1                   .00000E 00       .10000E-43       .00000E 00       .00000E 00
ZN 1                   .20000E-01       .20000E-01       .20000E-01       .20000E-01
ZN 1                   .00000E 00       .00000E 00       .00000E 00       .00000E 00

C  1                   .00000E 00       .10000E-19       .00000E 00
ZN 1                   .00000E 00       .00000E 00       .00000E 00
ZN 1                   .00000E 00       .00000E 00       .00000E 00


                  LOG10(MOLE FRACTION)   WEIGHT MATERIALS
AR 1                          -.018            38.35123
C  1                         -1.699              .24022
-  1                        -99.000              .00000
ZN 1                         -1.699             1.30760
ZN 1                        -99.000              .00000
C  1                        -99.000              .00000
ZN 1                        -99.000              .00000
ZN 1                        -99.000              .00000
TIME                1.338 SECONDS RETURNED          1338 MILLISECONDS USED
*STOP* 0
   0015    IC ANSWERS TO ME
TEMPERATURE = 3800.00 K    PRESSURE =     1.00 ATM

                         Y/MOLE
AR 1                   .96003E 00            38.35123
C  1                   .20000E-01              .24022
-  1                   .00000E 00              .00000
ZN 1                   .20000E-01             1.30760
ZN 1                   .00000E 00              .00000
C  1                   .00000E 00              .00000
ZN 1                   .00000E 00              .00000
ZN 1                   .00000E 00              .00000

TOTAL TIME USED WAS       1. SECONDS

***SOLGAS TERMINATED***
```

APPENDIX II - PROGRAMS USED FOR COMPUTER DATA ACQUISITION

A. Spectral-Line Intensity

The BASIC program shown below was used to acquire spectral-line intensities from three photomultiplier tubes. The acquisition routines were written in PDP-11 MACRO ASSEMBLER and linked with BASIC/RT-11 VOID using the following commands with the RT-11 V2 Linker:

```
*ADBAS = BASICR, FPMP.EIS, BASICE, BASICX/B:400/C
*FNTABL, ADCFN, GETADD, BASICH
```

User functions were implemented from BASIC by the use of the CALL statement.

1. Description of SCAN (A, B)

The array, passed as Argument A, accumulates data in the format specified by B. B (0, 0) is the number of channels to be used. A threshold value can be entered in B (1, 0) so that no values will be collected unless they are greater than the specified value. Data is acquired from each channel in a consecutive manner.

2. Description of DA 20 (A, B)

This function will display 118 data samples on two channels of a storage oscilloscope. The vertical amplifier on the scope should be set at 0.2 volts/
division and the time base should be set at 1 milli-second/division. TRIGGER MODE on NORM and SOURCE on LINE.

```
10 DIM A(121,0),B(1,0),C(11,11)
20 PRINT "ENTER FILE NAME ? ";\INPUT #0:F$
30 IF F$="" THEN 380
40 OPEN F$ FOR OUTPUT AS FILE VF1%(1180)
50 PRINT "ENTER THE NUMBER OF CHANNELS IN USE ? ";\INPUT #0:N
60 N=INT(N)
70 B(0,0)=N
80 K=0
90 PRINT "ENTER THE DESIRED THRESHOLD ?";\INPUT #0:T
100 T=INT(T)
110 B(1,0)=T
120 PRINT "SIGNAL FOR DATA ACQUISITION.......";\INPUT A$
130 IF A$<>"" THEN 380
140 FOR I=1 TO 10
150 FOR J=0 TO 121\A(J,0)=0\NEXT J
160 CALL "SCAN"(A,B)
165 CALL "DA20"(A,B)
170 GOSUB 280
180 PRINT "OK ?";\INPUT #0:A$
190 IF A$="Q" THEN 380
195 IF A$<>"Y" THEN 150
200 FOR J=1 TO 118
210 VF1(K+J)=A(J,0)
220 NEXT J
230 K=K+J
240 NEXT I
250 PRINT "ANY MORE ?";\INPUT #0:A$
260 IF A$="N" THEN 380
270 GO TO 20
280 FOR M=0 TO 20
290 PRINT A(M,0);TAB(10);A(M+20,0);
300 IF N<>3 THEN 310 \PRINT TAB(17);" | ";
310 PRINT TAB(20);A(M+40,0);
320 IF N<>2 THEN 330 \PRINT TAB(27)" | ";
330 PRINT TAB(30);A(M+60,0);
340 IF N<>3 THEN 350 \PRINT TAB(37)" | ";
350 PRINT TAB(40);A(M+80,0);TAB(50);A(M+100,0)
360 NEXT M
370 RETURN
380 CLOSE
```

If all X-values obtained are positive, they will be used as the new initial guess. If negative X-values appear, the difference between the initial and the calculated values is reduced in order to obtain positive values. For all substances with negative x-values, y_i^1 is put equal to zero where

$$y_i^1 = y_i + \lambda(x_i - y_i) \tag{8}$$

and λ is calculated.

In order to avoid too many iterations, it was found necessary to adopt a lowest allowed y-value. If the mole number for a substance becomes less than the lowest allowed (in this case, 10^{-75} mole), y_i is put equal to zero. That substance will then not be considered in the subsequent iterations as both X_i and y_i will be zero-valued. However, the iteration process is interrupted earlier if the condensed phases currently considered cannot exist together according to Gibbs phase rule.

When the improved, X approaches the guessed, Y mole numbers are becoming equal, the value of π_{l+1}, approaches zero. To achieve a satisfactory accuracy for all mole numbers, a value of π_{l+1} less than 10^{-8} is calculated. If the test is not satisfied, the calculated y-values are substituted into the equations (5), (7) and (6), and a new iteration cycle starts.

3. Use of the BASIC Program

A file is opened on disk with a name. If no file name is entered, the program will end. Enter the number of photomultipliers to be used. When data acquisition is desired, any key can be pushed except the RETURN which will terminate the program. The data acquired will be displayed on the oscilloscope screen and printed on the CRT screen. Then the user can either collect more data for the file or quit.

B. Data Reduction

Another BASIC program, not shown, was written to print out desired files and find the maximum intensity of each rotation. The program computed the averages and standard deviations for each channel of collected data.

APPENDIX IIIA - DERIVATION OF EQUATION FOR TEMPERATURE DETERMINATION USING THE TWO-LINE ATOM METHOD

A. Intensity of an Atom Line

The number of atoms (or molecules) dN spontaneously undergoing a transition from a higher state q to a lower state p during an interval of time dt is just:

$$dN = Nq\ Aqp\ dt \tag{1}$$

where Nq is the population of the state q and Aqp is the probability coefficient for the transition.

The intensity Iqp of an emission line is defined as the energy radiated per second. It is the product of the number of atoms of a species spontaneously undergoing a given transition in a second, and the energy of the photon released. The former is given by Equation (1), the latter by h Vqp. The resulting expression for Iqp is

$$Iqp = h\ Vqp\ Aqp\ Nq \tag{2}$$

If thermal equilibrium has been attained, Nq can be defined in terms of the Boltzmann distribution. In this case, population Nq can be related to the total population of the species in all states N by the expression

$$\frac{Nq}{N} = \frac{gq}{Z(T)}\ e^{-\ Eq/kT} \tag{3}$$

where gq is the statistical weight of the state q, and Z(T) is the quantum mechanical partition function for the species. In a representative system where few atoms are in an excited state, Z(T) = go, the statistical weight of the ground state.

Substituting Equation (3) in (2):

$$Iqp = h\ Vqp\ Aqp\ N\ \frac{gq}{go}\ e^{-Eq/kT} \qquad (4)$$

In all thermal sources; that is, in most flames, arcs and sparks at atmospheric pressure, the relative concentrations of atoms and ions are governed by thermal ionization equilibria. Consequently, the intensities of atom and ion lines vary considerably when the ionization equilibria is shifted. Ionization involves the form

$$na = (1 - \alpha)_n \qquad (5)$$

where α is in the degree of ionization on the total concentration (n) of the relevant element in the plasma.

Thus, the intensity of an atomic line depends upon the degree of ionization, the concentration of the element in the source as well as the absolute temperature, the Boltzmann content, the statistical weight, the frequency, the transition probability, and the excitation energy.

$$Iqp = n\,(1-\alpha)\,N\,e^{-Eq/kT}\quad Aqp\,\frac{gg}{go}\quad h\,Vqp \tag{6}$$

B. Temperature Determination Using Two Atom Lines

The absolute temperature T represents the equilibrium temperature. Calculations of the temperature can be made by determining the intensities of two lines of the same species. The lines must have unique energies, statistical weights, and probability coefficients. Lines a and b have emission intensities described by:

$$Ia = n\,(1-\alpha)\,N\,e^{-Ea/kT}\,Aa\,\frac{ga}{go}\,h\,Va \tag{7}$$

and

$$Ib = n\,(1-\alpha)\,N\,e^{-Eb/kT}\,Ab\,\frac{gb}{go}\,h\,Vb \tag{8}$$

Inserting $Va = C/\lambda a$, $Vb = C/\lambda b$ and taking the ratio of (7) and (8) results in:

$$\frac{Ia}{Ib} = \frac{n\,(1-\alpha)\,N\,e^{-Ea/kt}\,Aa\,\frac{ga}{go}\,h\,\frac{C}{\lambda a}}{n\,(1-\alpha)\,N\,e^{-Eb/kT}\,Ab\,\frac{gb}{go}\,h\,\frac{C}{\lambda b}} \tag{9}$$

Then canceling equivalent terms reduces Equation (9) to

$$\frac{Ia}{Ib} = \frac{e^{-Ea/kT}\,Aa\,ga\,\lambda b}{e^{-Eb/kt}\,Ab\,gb\,\lambda a} \tag{10}$$

Combining the exponential terms in Equation (10)

$$\frac{Ia}{Ib} = e^{-(Ea-Eb)/kT}\,\frac{Aa\,ga\,\lambda b}{Ab\,gb\,\lambda a} \tag{11}$$

The natural logarithm of Equation (11)

$$\ln\left[\frac{Ia}{Ib}\right] = \frac{-1}{T}\left[\frac{Ea-Eb}{k}\right] + \ln\left[\frac{Aa\ ga\ \lambda b}{Ab\ gb\ \lambda a}\right] \tag{12}$$

Solving for the absolute temperature, T

$$\frac{1}{T}\left[\frac{Ea-Eb}{k}\right] = \ln\left[\frac{Aa\ ga\ \lambda b}{ab\ gb\ \lambda a}\right] - \ln\left[\frac{Ia}{Ib}\right] \tag{13}$$

$$\frac{1}{T} = \frac{\ln\left[\frac{Aa\ ga\ \lambda b}{Ab\ gb\ \lambda a}\right] - \ln\left[\frac{Ia}{Ib}\right]}{\left[\frac{Ea-Eb}{k}\right]} \tag{14}$$

$$T = \frac{\left[\frac{Ea\ -\ Eb}{k}\right]}{\ln\left[\frac{Aa\ ga\ \lambda b}{Ab\ gb\ \lambda a}\right] - \ln\left[\frac{Ia}{Ib}\right]} \tag{15}$$

Converting to Base 10 logarithm

$$T = \frac{\left[\frac{Ea\ -\ Eb}{k}\right]}{+2.303\ \log\left[\frac{Aa\ ga\ \lambda b}{Ab\ gb\ \lambda a}\right] - 2.303\ \log\left[\frac{Ia}{Ib}\right]} \tag{16}$$

$$T = \frac{\frac{1}{+2.303\ k}\left[Ea\ -\ Eb\right]}{\log\left[\frac{Aa\ ga\ \lambda b}{Ab\ gb\ \lambda a}\right] - \log\left[\frac{Ia}{Ib}\right]} \tag{17}$$

where: K = Boltzmann Constant (8.617×10^{-5} eV•K^{-1})

E = Excitation Energy (eV)

Equation (17) simplifies to

$$T = \frac{5040\ (Ea\ -\ Eb)}{\log\left[\frac{Aa\ ga\ \lambda b}{Aa\ gb\ \lambda a}\right] + \log\left[\frac{Ib}{Ia}\right]} \tag{18}$$

APPENDIX IIIB - DERIVATION OF EQUATION FOR DETERMINATION OF UNCERTAINTY IN TEMPERATURE RESULTS

The temperature is calculated from one experimentally determined quantity, the intensities of two spectral lines. The ratio of emission intensities for two spectral lines was given in Appendix IIIC, Equation (12), by the expression

$$\ln \frac{Ia}{Ib} = -\left[\frac{Ea - Eb}{kT}\right] + \ln \left[\frac{A1g1\,\lambda 2}{A2g2\,\lambda 2}\right] \qquad (1)$$

Differentiating on both sides with respect to T:

$$\frac{1}{Ia/Ib} \quad \frac{d\,(Ia/Ib)}{dT} = \frac{Ea - Eb}{kT2} \qquad (2)$$

Solving for dT:

$$dT = \frac{kT2}{Ea - Eb} \quad \frac{d\,(Ia/Ib)}{Ia/Ib} \qquad (3)$$

the absolute error in temperature, eT is

$$eT = \frac{kT2}{Ea - Eb} \quad \frac{e\,(Ia/Ib)}{Ia/Ib} \qquad (4)$$

and the relative (or fractional) error in temperature is

$$\frac{eT}{T} = \frac{kT}{Ea - Eb} \quad \frac{e\,(Ia/Ib)}{Ia/Ib} \qquad (5)$$

where $k = 8.617 \times 10^{-5}$ eV/deg.